Article

Current Biology

# Evolution at multiple processing levels underlies odor-guided behavior in the genus *Drosophila*

## Graphical abstract

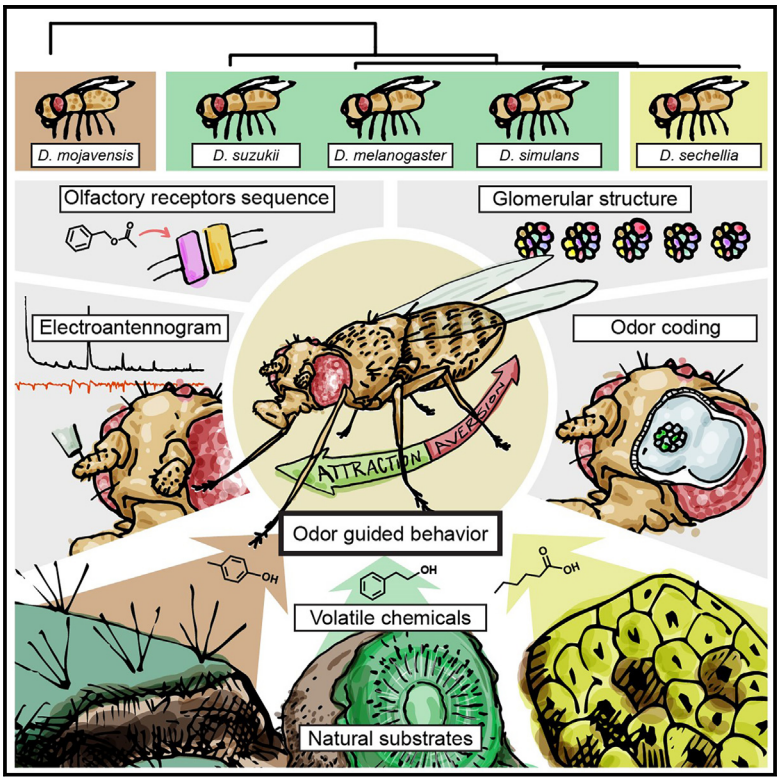


## Highlights

- *Drosophila* flies detect a diverse range of host plant and non-host plant odorants
- The same odorants can have different valences in different species
- Differences in odor coding and behavior depend on phylogeny and the species' ecology

## Authors

Ana Depetris-Chauvin, Diego Galagovsky, Ian W. Keesey, Bill S. Hansson, Silke Sachse, Markus Knaden

## Correspondence

ssachse@ice.mpg.de (S.S.), mknaden@ice.mpg.de (M.K.)

## In brief

By comparing five *Drosophila* species that differ in their phylogenetic distance from each other and the similarity of their ecological niche, Depetris et al. show that both phylogeny and the ecological niche are key factors in the evolution of olfactory receptors, antennal lobe structures, odor coding, and behavior in drosophilid flies.

Depetris-Chauvin et al., 2023, Current Biology *33*, 4771–4785
November 20, 2023 
https://doi.org/10.1016/j.cub.2023.09.039

CellPress

Current Biology

CellPress

Article

# Evolution at multiple processing levels underlies odor-guided behavior in the genus *Drosophila*

Ana Depetris-Chauvin,[1,2,3,4] Diego Galagovsky,[1,3] Ian W. Keesey,[1,5] Bill S. Hansson,[1] Silke Sachse,[2,6,7,*] and Markus Knaden[1,6,8,9,*]

[1]Max Planck Institute for Chemical Ecology, Department of Evolutionary Neuroethology, 07745 Jena, Germany
[2]Research Group Olfactory Coding, Max Planck Institute for Chemical Ecology, 07745 Jena, Germany
[3]These authors contributed equally
[4]Present address: Microbiome Dynamics Department, Leibniz Institute for Natural Product Research and Infection Biology-Hans Knöll Institute, 07745 Jena, Germany
[5]Present address: School of Biological Sciences, University of Nebraska, Lincoln, NE 68588, USA
[6]Senior author
[7]X (formerly Twitter): @SilkeSachse
[8]X (formerly Twitter): @mknaden1
[9]Lead contact
*Correspondence: ssachse@ice.mpg.de (S.S.), mknaden@ice.mpg.de (M.K.)
https://doi.org/10.1016/j.cub.2023.09.039

## SUMMARY

Olfaction is a fundamental sense guiding animals to their food. How the olfactory system evolves and influences behavior is still poorly understood. Here, we selected five drosophilid species, including *Drosophila melanogaster*, inhabiting different ecological niches to compare their olfactory systems at multiple levels. We first identified ecologically relevant natural food odorants from every species and established species-specific odorant preferences. To compare odor coding in sensory neurons, we analyzed the antennal lobe (AL) structure, generated glomerular atlases, and developed GCaMP transgenic lines for all species. Although subsets of glomeruli showed distinct tuning profiles, odorants inducing species-specific preferences were coded generally similarly. Species distantly related or occupying different habitats showed more evident differences in odor coding, and further analysis revealed that changes in olfactory receptor (OR) sequences partially explain these differences. Our results demonstrate that genetic distance in phylogeny and ecological niche occupancy are key determinants in the evolution of ORs, AL structures, odor coding, and behavior. Interestingly, changes in odor coding among species could not be explained by evolutionary changes at a single olfactory processing level but rather are a complex phenomenon based on changes at multiple levels.

## INTRODUCTION

Changes in environmental conditions exert selective pressure on organisms and can lead to novel evolutionary traits. Sensory systems are at the interface between the environment and the animal's internal physiology and behavior. They determine how animals perceive and understand the world, a concept known as the "animal umwelt" after Jakob von Uexküll's theory.[1] It is unsurprising, then, that the evolution of sensory systems underlies adaptative behaviors in the light of environmental changes or occupation of new ecological niches.[2–4] Rapid changes in the vestibular system of early cetaceans occurred during the transition from land to marine environments and allowed the fast body rotation mode of cetacean locomotion.[5] Repetitive exposure to glucose in toxic baits led to changes in taste neurons and the subsequent emergence of an adaptative aversion to glucose in German cockroaches.[6] Adaptations in taste, olfaction, and mechanosensation have been shown to accompany behavioral adaptations to new ecological niches in the *Drosophila* genus.[7–9] Despite these insightful case studies, how changes in sensory systems drive behavioral change at a more global scale is still poorly understood.

The olfactory system of different *Drosophila* species is an excellent model to study how changes in sensory systems drive behavioral evolution. Originally from the tropics, *Drosophila* flies underwent several rounds of radiation that resulted in more than 2,000 species present in all sorts of habitats and exploiting a wide range of resources.[10,11] Some, like the model organism *Drosophila melanogaster*, lay eggs in fermenting fruits and feed upon the microbial community present in the fruit.[11–13] Other species have evolved to feed on flowers, cacti, mushrooms, flux, or other plant parts. Although most species are considered generalist, several have specialized in the use of a specific host; for example, *D. sechellia* uses noni fruit, which is toxic to other flies.[7,11,14] In this wide range of habitats, *Drosophila* species are exposed to different chemical stimuli, and the success of each species depends on correctly deciphering its chemical environment and exhibiting appropriate behaviors toward

relevant odorants. Detection of key ecologically relevant odorants drives adaptative behaviors such as foraging, avoidance of toxic substrates, the search for a mating partner, oviposition site selection, and others.[15–17]

Volatile chemicals are detected in the fly antenna and maxillary palps by olfactory sensory neurons (OSNs) harbored in porous hair-like structures or sensilla. The direct detection of odorants is carried out by specific olfactory receptors (ORs) or ionotropic receptors (IRs) in the OSN dendrites, in combination with a coreceptor (Orco for ORs and Ir8a, Ir25a, or Ir76b for IRs).[18,19] The axons of OSNs transmit the olfactory information to the first olfactory brain structure, the antennal lobe (AL), where OSNs expressing the same OR IR converge in a specific region known as a glomerulus. The OSN signal is processed in the glomerular array by local interneurons, after which the odor information is transmitted to the lateral horn and the mushroom bodies via projections neurons.[20–23]

Several studies have focused on the role of OR divergence as a driver of behavioral shift across species. Indeed, OR genes are evolving unusually rapidly compared with other genes, and ecological specialization influences OR gene repertoires in mammals and flies.[24–30] Changes in OR tuning, OR loss and diversification, and changes in OSN numbers are correlated and are probably responsible for the change of odor coding to certain chemicals across *Drosophila* species.[14,28,29,31–38] It is noteworthy that these comparative studies of olfactory responses are either limited to the detection of a few odorants, focused only on one pair of species, or lack the link to behavior. Consequently, how olfactory systems are evolving on a larger scale within the *Drosophila* genus and what behavioral consequences these changes have are still poorly understood and will be the focus of this work.

Here, we followed a multi-disciplinary approach to study the evolution of the olfactory systems of five *Drosophila* species exploiting different ecological niches. We focused both on generalists (*D. melanogaster*, *D. simulans*, and the agricultural pest *D. suzukii*) and specialists (*D. sechellia* and *D. mojavensis*). We tested their behavioral preferences toward a large set of odorants that we identified in their different natural feeding substrates or hosts. We next generated morphological atlases of the first olfactory processing center, i.e., the AL of the non-*melanogaster* species. Finally, we developed genetic tools to express the calcium indicator GCaMP6f under the *Orco* promoter and performed *in vivo* functional imaging recordings in all species. We found species-specific differences regarding the valence of odorants, i.e., their attractiveness or aversiveness, which often correlated with the species' preferences for the different hosts.

Interestingly, although these species also exhibit differences in the peripheral coding of some odorants, the coding of many odorants, even those that underwent a dramatic change of valence, is, to a certain extent, conserved. Finally, we discovered that evolutionarily closely related species or species sharing ecological niches show more similarities at all levels analyzed in the present study, from OR sequences, the odor coding and AL structure, all the way to the behavioral responses. Our results show that evolutionary distance and niche specialization are both critical determinants of odor coding, glomerular structure, and behavioral divergence between species.

## RESULTS

### *Drosophila* flies detect a diverse range of host plant and non-host plant odorants

In order to study how different species of flies detect and respond to ecologically relevant odorants, we selected five *Drosophila* species exploiting different or similar host plants and with a wide range of evolutionary distances (Figure 1A). We studied the genetic model organism *D. melanogaster* and its close relatives *D. simulans* (a generalist on fermented fruit like *D. melanogaster*) and *D. sechellia* (a specialist on the noni fruit *Morinda citrifolia*).[11] We also investigated the pest species *D. suzukii*, which exploits both fresh and fermented fruit,[39] and, as the most distantly related species of our study, *D. mojavensis wrigleyi* specialized in the prickly pear cactus (*Opuntia* cacti[40]). To simplify, we further refer to *D. mojavensis wrigleyi* as *D. mojavensis*.

We first identified the chemical composition of headspace extracts of the host plants by gas chromatography followed by mass spectrometry (GC-MS) (Figure 1B). As a representative of fermented fruit, we chose fermented kiwi, which was previously reported to be highly attractive for *D. melanogaster* adult flies.[42] The composition of headspace extracts differed significantly. Fermented kiwi volatiles consisted of esters, alcohols, and, to a lesser extent, terpenes. The headspace obtained from the noni fruit contained mainly acids and esters, while fermented stems of prickly pear cactus presented an immense variety of benzene derivatives and other complex compounds (Figure 1C; Table S1).

Next, we performed GC coupled with electroantennographic detection (GC-EAD) to establish which specific volatiles are detected by the antenna of each of the five species. Flies did not only respond to specific compounds emanating from their own preferred host plant but were also able to detect chemicals coming from other species' hosts. Although one could have speculated that specialist flies tune their olfactory sense to those odorants emanating from their hosts, all species were strikingly able to detect similar odorant sets with their antennae (Figure 1D). Overall, while all species detected a lower percentage of kiwi odorants (28% of identified odorants compared with 50% and 45% of odorants detected from noni and cactus, respectively), responses to kiwi odorants were stronger. Interestingly, EAD responses to methyl hexanoate, a key noni odorant, were exceptionally high in *D. sechellia*, while responses to p-cresol, the most abundant chemical in the cactus headspace, were significantly higher in *D. mojavensis* (Figure S1).

### Specific odorants can have different valences in related species

Using a binary-choice trap assay, we investigated olfactory behavioral responses toward headspace extracts in the five species. Briefly, 50 flies were released into a small container, where they could freely choose between two small traps, one containing a headspace extract and the other solvent (details in the STAR Methods section). Flies of each species were attracted to the headspace extracts from their preferred host plants, as well as to those of other host plants, except for the cactophilic species *D. mojavensis*, which was only highly attracted to the fermented cactus stems (Figure 2A).

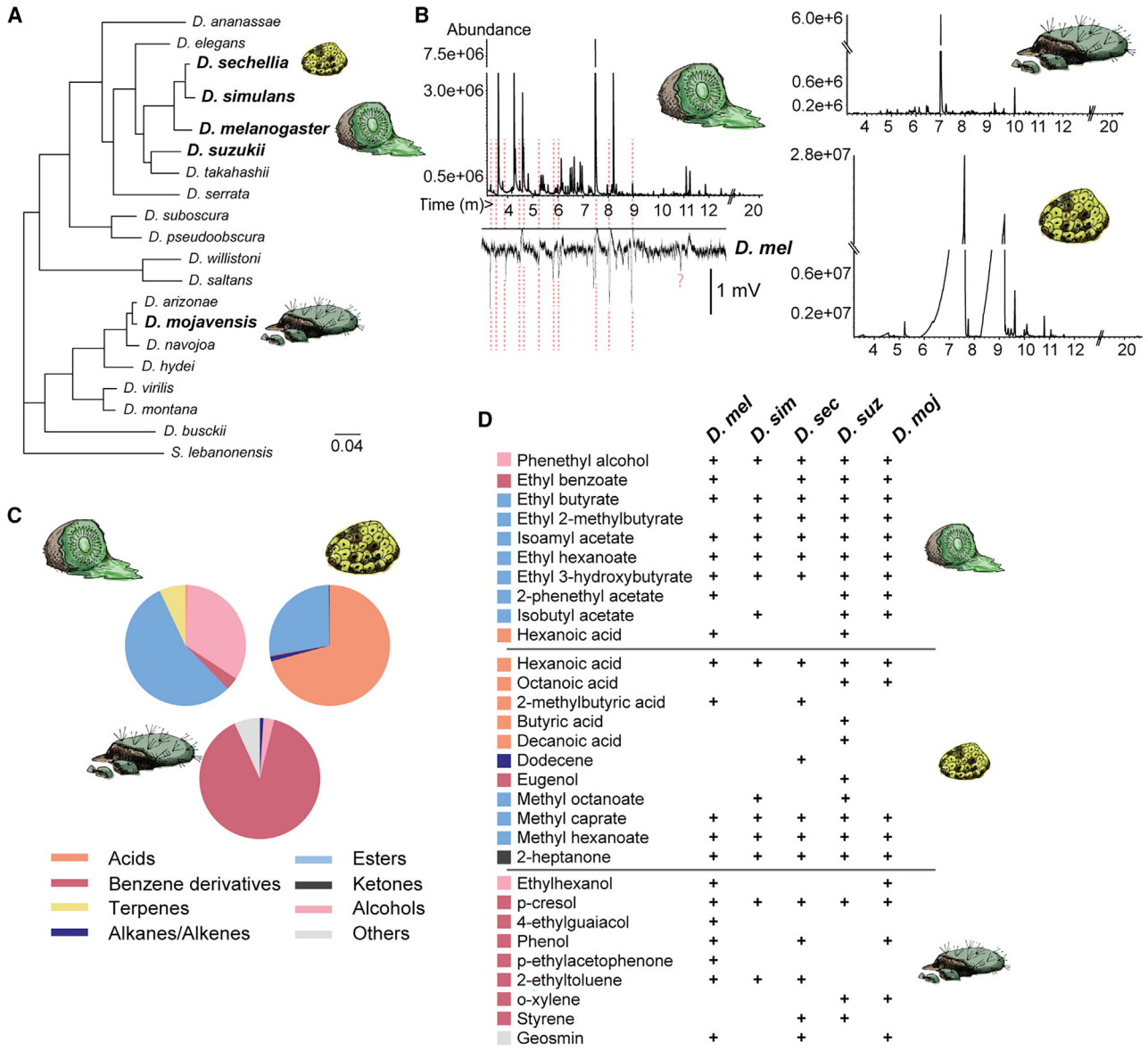


**Figure 1. Chemical profiles and antennal responses to host odorants**

(A) Phylogenetic tree highlighting the five species used in this study and their preferred host plants, based on the complete genome of 19 selected *Drosophila* species and one outgroup, *Scaptodrosophila lebanonensis*.[41] Maximum likelihood (ML) phylogenetic analyses displayed strong ultrafast bootstrap support. Scale bars, 0.04 nucleotide substitutions per site.

(B) GC-MS traces from volatile collections obtained from fermented kiwi, noni fruit, and prickly pear cactus stems. A representative electroantennogram trace from *D. melanogaster* simultaneously recorded with the GC run of fermented kiwi is depicted below the left chromatogram. The dotted lines point to the volatiles eliciting a response in the fly's antenna. (?) indicates a response not present in all recordings and could not be attributed to any volatile in the GC traces.

(C) Chemical composition of volatile collections of kiwi, noni, and cactus samples.

(D) List of volatiles detected in the headspace samples by all five species. The odorants in the list correspond to those that elicited a GC-EAD response that could be further confirmed by EAD applying individual chemicals in the corresponding concentration (see STAR Methods).

See also Figure S1 and Table S1 for a complete list of chemicals identified in the volatile collection samples.

Next, we sought to unravel the valence of individual odorants emanating from the host plants, as well as the valence of other ecologically relevant odorants previously studied.[39,43,44] In total, we screened 39 odorants in the five species and found attractive, neutral, and aversive odors for all species (attractive:aversive ratios, 18:5 in *D. melanogaster*, 9:10 in *D. simulans*, 9:10 in *D. sechellia*, 7:7 in *D. suzukii*, and 9:4 in *D. mojavensis*). Consistent with the general attraction to kiwi headspace extracts, all species found a majority of odorants emanating from fermented kiwi attractive or neutral. On the contrary, a higher proportion of chemicals emitted by noni fruit and cactus elicited aversion, except in *D. melanogaster* and *D. sechellia*, which showed

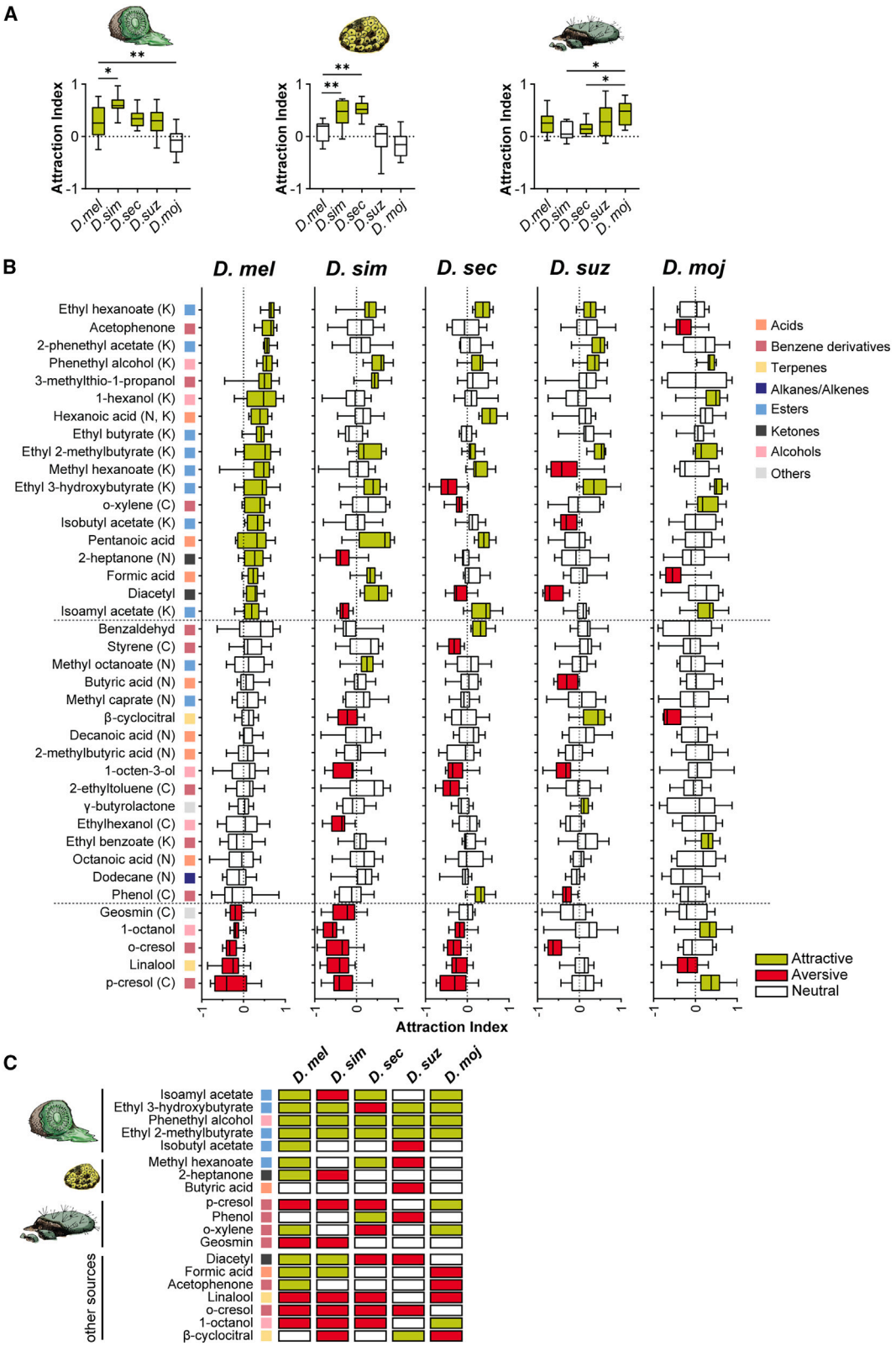


**Figure 2. Related *Drosophila* species can exhibit opposite valences toward ecologically relevant odorants**

(A) Attraction indices of five fly species toward volatile collections from fermented kiwi, noni, and prickly pear cactus. Attraction indices were calculated as (number of flies in odor trap − number of flies in control trap)/total number of flies in both traps. All odor collections were attractive (green boxes) or neutral (white

*(legend continued on next page)*

attraction to some noni odorants, and *D. mojavensis*, which was highly attracted to the most abundant cactus compound, p-cresol (Figures 2B and S2).

Our behavioral screen, which spans chemicals from different chemical groups and ecological origins, unveiled some exciting differences in interspecies. Although some odorants showed the same valence, e.g., the generally attractive odorant phenethyl alcohol, several others displayed opposite valences across species, e.g., ethyl 3-hydroxybutyrate, which was attractive for most species but aversive for *D. sechellia*. Furthermore, even closely related and ecologically similar species like *D. melanogaster* and *D. simulans* exhibited opposing preferences for some odorants, such as 2-heptanone and isoamyl acetate (Figures 2B and S2B; Table S2).

To simplify further analyses, we selected a subgroup of 19 odorants from our screen and continued studying the odor perception mechanisms using *in vivo* functional imaging of the AL. The subgroup included attractive and aversive odorants for each species, key odorants from host plants or of ecological relevance, and odorants with equal or opposite valence between species (Figure 2C). These odorants were carefully selected to test several hypotheses: odor coding of attractive vs. aversive odors in each species, cross-species coding conservation of odors with equal or opposite valence, and odor coding conservation of ecologically relevant odors.

## AL atlases of non-*melanogaster* species

As a next step, we investigated how odors are detected by OSNs in different species. To be able to perform functional calcium imaging at the level of the first olfactory neuropil, the AL, in the non-*melanogaster* species, we generated transgenic lines expressing the calcium indicator GCaMP6f in all OSNs harboring the coreceptor Orco. We opted to generate these lines using the UAS-GAL4 binary transcriptional system to provide genetic tools useful for the broad community studying these four non-*melanogaster* species.

We generated *Orco*-GAL4 and UAS-GCaMP6f lines for all species, with the exception of *D. simulans* UAS-GCaMP6s, which was previously generated[45] and generously donated for our study. All our Orco>GCaMP lines showed specific and clear expression in the AL (Figure 3A) and responded to odorant puffs in a specific manner (Figure 4).

Before studying the odorant-evoked responses at the level of OSN terminals, we analyzed the glomerular structure in the different species. We performed AMIRA-based AL reconstructions of NC82-stained brains of each species (wild-type [WT] strains), and identified and named all glomerular structures in the AL. As a reference, we used the previously reconstructed brains of *D. melanogaster* and named the glomeruli based on their relative position in the AL, as it was originally done in *D. melanogaster*.[46] Certain glomeruli's characteristic shape and position, e.g., D, DA1, DM2, VA2, V, DP1m, and others, facilitated the reconstruction and provided landmarks to compare the overall structure of the AL of different species. In addition, we identified glomeruli innervated by Orco$^+$ OSNs by performing glomerular reconstruction on Orco>GCaMP brains (Figure 3; Table S3). We generated digital AL atlases for each species (for a 3D reconstruction of all atlases, see https://doi.org/10.17617/3.ZWVXDX), which facilitated the identification of responsive glomeruli in our subsequent functional imaging experiments (for the identification and naming of non-*melanogaster* glomeruli, see STAR Methods). Our digital AL atlases represent an essential tool for future studies of the AL of any of the here-described non-*melanogaster* species.

The overall structure of the ALs was remarkably similar between species, although the AL size and its relative volume compared with the whole brain differed significantly between species, and three and four novel glomeruli were identified in *D. suzukii* and *D. mojavensis*, respectively (Figures S3A and S3B; Table S3). We found sex-specific differences in glomerular volume in *D. melanogaster* for the FruM$^+$ glomeruli DA1, VA1d, VA1v, and VL2a, consistent with previously reported data.[47] We observed the same differences in the homologous glomeruli in *D. simulans*, while in other species, we only found sex differences in the volumes of *sec*DA1, *suz*VA1d, and *moj*VL2a from *D. sechellia*, *D. suzukii*, and *D. mojavensis*, respectively (Figure S3C).

Consistent with previous reports, we observed a significantly increased volume in the DM2, VM5d, DL2d, and DL2v, and a decreased volume in DP1m, of *D. sechellia*[28,37,48] compared with that of *D. melanogaster*. We also found several further changes in other glomeruli and species (Figure 3B; Table S3). Of note, we observed an increase of *suz*DM4 and *suz*DM5 and a decrease in *suz*DM2 in *D. suzukii*, glomeruli that we previously demonstrated to be innervated by antennal basiconic sensilla type 2 (ab2) and ab3-harbored OSNs. As expected, these size changes correlated with a higher proportion of ab2 than ab3 sensilla in *D. suzukii*.[31]

## Functional imaging in the AL of *Orco*>GCaMP6 transgenic lines reveals different degrees of conservation in odor coding between species

We next performed functional calcium imaging in the AL of *Orco*>GCaMP6 flies of the five species, and we identified

boxes), and significant differences were observed between species (one factor ANOVA, post-test Tukey, *$p < 0.05$, **$p < 0.01$. n = 5–14 independent replicates). For simplicity, only significant differences with *D. melanogaster* (for kiwi), *D. sechellia* (for noni), or *D. mojavensis* (for cactus) are shown. Headspace collections were diluted at 1:5 (kiwi), 1:10 (cactus), or 1:100 (noni) in mineral oil. Boxplots depict median responses, interquartile ranges, and maximum and minimum values.

(B) Attraction indices of five fly species for 39 single odorants corresponding to those identified in Figure 1D plus ecologically relevant odorants already described before (see main text). K, N, and K at the end of the chemical name stand for odorants emanating from kiwi, noni, and cactus headspaces, respectively. Odorants are ordered by increasing index value according to responses in D. melanogaster, and the color code indicates the chemical group explained in the figure. n = 8–12 independent replicates. Single odorants were tested at a concentration of $10^{-3}$, except for geosmin, which was tested at $10^{-4}$. Boxplots depict median responses, interquartile ranges, and maximum and minimum values.

(C) List of odorants selected for further analysis.

In all figures, box plots give the median, 25%–75% quartiles, and the minimum and maximum values, and light green, white, and red indicate attractive, neutral, and aversive odorants, respectively (attraction index statistically significant >0, =0, or <0, t test).

See also Figure S2 and Table S2 for a complete list of the behavioral indices calculated for all species/odorants.

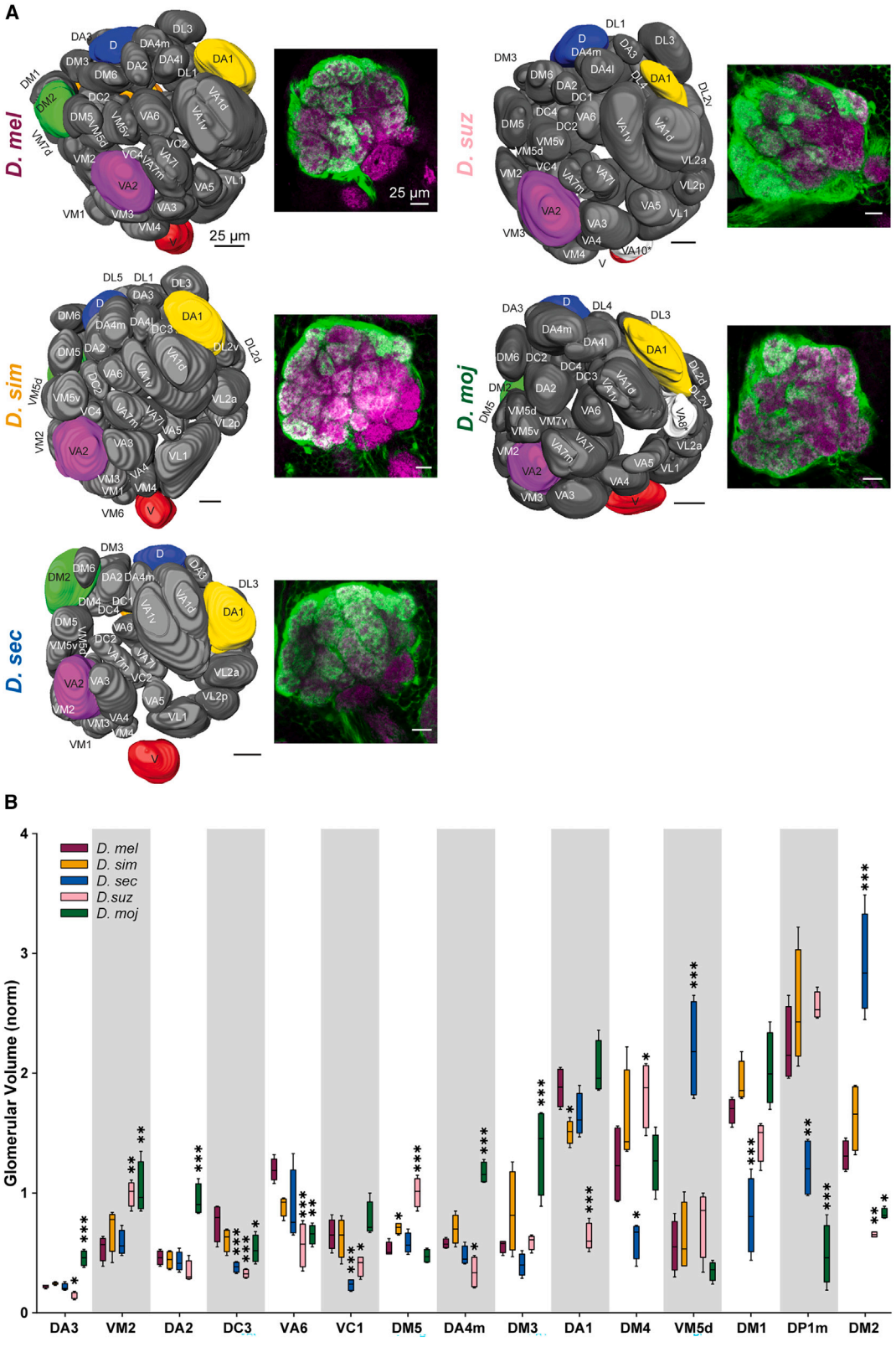


**Figure 3. Antennal lobe reconstructions of all species**

(A) Left, frontal view of antennal lobe reconstructions of each species. Right, a single-plane image of Orco>GCaMP line (magenta, NC82; green, GFP). The scale line represents 25 μm in all images.

*(legend continued on next page)*

responsive glomeruli to all odorants in our panel of 19 odorants. In our preparation, we reliably identified 24 Orco$^+$ glomeruli (Figure 4A), representing approximately 60% of the total Orco$^+$ glomeruli. Most odorants elicited neuronal responses combinatorially in all species by activating several glomeruli. Hence, we will refer to the glomerular activation pattern in response to an odorant as the odor coding. A clear exception to the multiglomerular activation pattern was geosmin, which activated only the DA2 glomerulus in most species (Figure 4).

As a first step, we analyzed the coding similarity of different odorants within each species (Figure S4A). In particular, we asked whether odorants with a similar valence are more similarly coded than odorants with a different valence. We indeed found such a difference in *D. melanogaster* (Figure S4B), although a cluster analysis revealed no clear separation between attractive and aversive odors (Figure S4C), consistent with a previous study from our group.[43] In all other species, no clear separation between odorants with different valences was observed (Figures S4B and S4C).

As a next step, we compared the odor coding between species, considering whether the odorant valence was equal or opposite across species. When performing a pairwise comparison between species, we did not find significant differences between the level of odor coding similarity (e.g., correlation of odor coding) of odorants with equal or opposite valence across species for any of the tested species pairs (Figure S5A; see STAR Methods for details on the analysis). One could expect that specialist species have evolved more pronounced changes in odor coding for the chemicals emanating from their host, compared with the coding toward odorants from other sources. To our surprise, this was not the case for the two specialists in this study, *D. sechellia* and *D. mojavensis*. In general, we did not find significant differences in the levels of odor coding conservation between odorants emitted from the different host plants (Figure S5B). These results encouraged us to study the odor coding for each individual odorant across different species in more detail. In particular, we wondered whether specific odorants show conservation of odor coding across species and, vice versa, whether specific odorants show clear changes in odor coding for some species.

When we took a closer look at the coding of individual odorants in the different species, certain odorants, e.g., geosmin or ethyl 3-hydroxybutyrate, showed a high degree of coding conservation (Figure 5A). *D. mojavensis* differed slightly from other species due to a significantly increased response of *moj*DA2 to geosmin (Figure 5B), a glomerulus that is twice as big in the cactophilic species compared with the other four species (Figure 3B). Other odorants, however, like 1-octanol and o-xylene, differed significantly regarding which glomeruli they activated (Figure 5A) in different species. The coding of some odorants, like two odorants emanating from kiwi samples (phenethyl alcohol and ethyl 2-methyl butyrate), was conserved within the species belonging to the *D. melanogaster* subgroup but differed in the more distantly related species *D. suzukii* in the case of phenethyl alcohol and *D. mojavensis*, in the case of ethyl 2-methyl butyrate (Data S1). In addition, in some cases, we observed that the relative activation of glomeruli differed between species, resulting in a shift of the best-responding glomeruli. For example, the leaf odor β-cyclocitral strongly activated the VC1 glomerulus in *D. melanogaster*, while in *D. suzukii* the best-responding glomerulus was *suz*DM2, consistent with its detection in ab3A neurons in that species.[31] Also, the noni odorant methyl hexanoate activates the DM3 glomerulus strongly in *D. melanogaster* and, to a lesser extent, DM2 and VM5d, while in *D. sechellia* the detection of this compound is shifted toward *sec*DM2, to the detriment of *sec*DM3 activation (Data S1).

In conclusion, our functional imaging experiments in these five *Drosophila* species revealed different degrees of odor coding conservation between them. Interestingly, changes in odor coding in OSN terminals could neither be predicted by the change in valence across species nor could it be considered a global specialization toward the detection of volatiles of a given species' host.

## Evolutionary distance and niche occupancy could explain the evolution of olfactory systems at multiple levels

So far, we have analyzed the differences in odor-guided behavior (Figure 2), AL structure (Figure 3), and primary detection of odorants (Figures 4 and 5). Next, we studied the changes in OR sequences. We calculated the evolutionary distances in OR sequences (Table S4) and generated phylogenetic trees using all OR sequences, as well as the sequence of ORs that would putatively innervate the glomeruli studied here. As previously reported,[34,49] we observed multiple cases of OR loss and OR duplication in *D. mojavensis* and *D. suzukii* (Figures 6A and S6).

Overall, OR sequences within the *D. melanogaster* species subgroup, i.e., *D. melanogaster*, *D. simulans*, and *D. sechellia*, were more similar to each other than those of the more distantly related species *D. suzukii* and *D. mojavensis* (Figure 6B). This was also true for behavioral, glomerular volume, and odor coding distances (Figures 6C–6E). Moreover, although *D. simulans'* closest relative is *D. sechellia*, the neuronal responses to our panel of odorants were more similar between *D. melanogaster* and *D. simulans*, two species sharing more similar ecological niches than *D. simulans* and *D. sechellia*. Notably, the same was observed in terms of the OR sequence, behavioral responses, and the changes in glomerular volume, suggesting that niche specialization, as well as time (evolutionary distance), are both strong determinants of receptor sequencing, odor coding, glomerular structure, and behavioral divergence among different species (Figures 6B–6E).

## Changes in OR sequence correlate with changes in odor tuning of corresponding glomeruli

Finally, to compare the responses of individual glomeruli between species, we analyzed the correlation of the responses in each of the 24 glomeruli using our panel of 19 odorants,

(B) Glomerular volume (normalized by total antennal lobe volume) of those glomeruli with the most drastic volume changes between species (at least a duplication or reduction to a half of the glomerular volume). All species were compared with *D. melanogaster*. (One-way ANOVA followed by Dunnett's post hoc test, *$p < 0.05$, **$p < 0.01$. n = 4–6 independent antennal lobes.) Boxplots depict median responses, interquartile ranges, and maximum and minimum values. See also Figure S3 and Table S3.

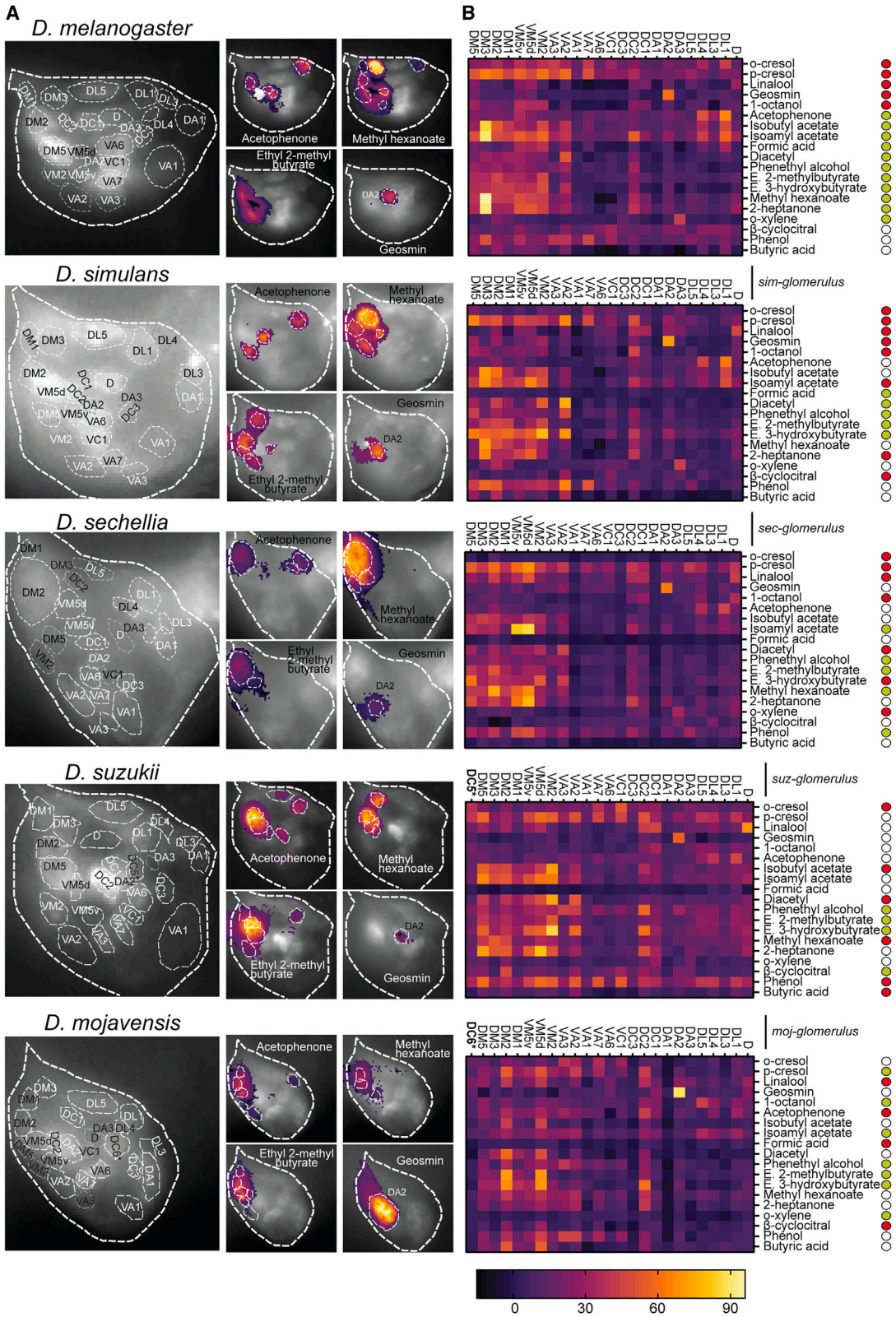


**Figure 4. Identification of responsive glomeruli by in vivo functional imaging of Orco>GCaMP6 transgenic lines**

(A) Representative images of Orco>GCaMP6 flies of the five species. Left: wide-field fluorescent images of Orco>GCaMP6 lines labeling glomeruli analyzed (gray dashed lines are glomeruli recorded from a different focal plane). Right: representative images of odor responses to four selected odorants. False color-code

*(legend continued on next page)*

comparing *D. melanogaster* with the other four species. Glomerular activity differed more between *D. melanogaster* and *D. mojavensis* (Figure 7A), as was expected given the high phylogenetic distance between these two species.

Gene sequence changes can modify the tuning of ORs.[28,29,50] In addition, gene duplication could lead to receptors detecting new ligands, while pseudogenization could cause the loss of function of certain receptors. All these modifications at the OR sequence level could ultimately change ORs' tuning to their respective odor ligands and subsequently lead to changes in the odor code at the AL level. Therefore, we decided to compare the degree of conservation in glomerular activity with the changes in OR sequences between species. Remarkably, we found a strong negative correlation between the evolutionary distance of OR sequences and the conservation of glomerular activity across species (Figure 7B), suggesting that changes in OR sequence could be partially responsible for the changes in odor coding we observed in our study.

## DISCUSSION

How sensory systems evolve and influence behavioral changes across species is one of the long-standing questions in evolutionary neuroethology. Here, we studied how the olfactory systems of five *Drosophila* species differ at multiple levels, i.e., the evolution of ORs, the peripheral detection of odorants, the structure of and olfactory coding at the AL, and, ultimately, the odor-guided behavior, all in the context of ecologically relevant odorants. Although some odorants trigger similar behaviors across species, we observed that some specific chemicals differ in valence. By implementing genetically expressed calcium sensors in non-*melanogaster* species, we demonstrated that behavioral shifts cannot always be explained by drastic changes in the primary detection of odorants, i.e., changes in the neuronal responses of OSNs' axonal terminals. Moreover, changes in primary odor coding across species might be partially due to sequence changes in their respective OR genes.

Our global comparative analysis revealed that species that share ecological niches—or are more closely evolutionarily related—are more similar at all levels, from OR sequences, odor coding, and AL structure to the behavioral level. Our results highlight the key role of phylogeny as well as ecological niche in shaping the olfactory systems and odor-guided behavior of *Drosophila* flies.

### Responses to host plant odorants

Our goal was to study the olfactory system of different species in controlled laboratory conditions while simultaneously analyzing stimuli with an ecological meaning. Although we could not use the exact concentrations present in the plant headspaces for technical reasons, we used odorants at relatively low concentrations ($10^{-3}$ and $10^{-4}$) for our behavioral and functional imaging experiments. Previous studies used higher concentrations; consequently, their conclusions might not be easily transferable to a more ecological situation.[28,29,43]

Among the ecologically relevant odorants tested in our study, we found that diacetyl, a byproduct of alcoholic fermentation,[16] is attractive to *D. melanogaster* and *D. simulans* but aversive to *D. suzukii*. All three species are attracted to fermenting fruit,[39] but gravid *D. suzukii* females avoid fermenting substrates to oviposit in fresh fruit specifically. Furthermore, *D. suzukii* adults are less resistant to alcohol,[51] so aversion toward diacetyl could protect *D. suzukii* flies from toxic alcohol levels in fermenting fruit.

The olfactory system of *D. sechellia* is tuned to the detection of noni odorants, particularly to the attractive odorants methyl hexanoate and hexanoic acid.[37] Interestingly, two of the most abundant chemicals in our noni samples, i.e., octanoic acid and methyl octanoate, neither elicited strong responses in the antenna (Figure 1D; Table S1) nor showed attraction in our behavioral assays (Figure 2B). Although the increased sensitivity to hexanoic acid appears to be mediated by changes in IRs,[28] changes in the tuning of OR22a$^{+}$-OSNs, innervating the *sec*DM2 glomerulus, are responsible for the increased sensitivity to methyl hexanoate and are, at least partially, responsible for the attraction toward this odorant.[29] We confirmed this increase in *sec*DM2 sensitivity to methyl hexanoate in *D. sechellia*, and we also noticed that the responses in *sec*DM3, whose corresponding glomerulus in *D. melanogaster* is highly responsive to methyl hexanoate, were significantly lower (Data S1).

The most prominent chemical found in the fermented cactus samples was p-cresol, which elicited attraction in *D. mojavensis* but repulsion in the other species (Figure 2B; Table S1). Overall, detection of p-cresol was similar among species, but minor changes in specific glomeruli (DM3, DM5, VM2, and VM5v) were still observed in *D. mojavensis* (Data S1). Another interesting compound found in the cactus sample was geosmin, a chemical with a characteristic earthy smell produced by *Penicillium* fungi and some bacterial species. *D. melanogaster* flies are very sensitive to the smell of geosmin, detecting it in small quantities via a dedicated olfactory pathway and responding with diverse aversive behaviors.[52] Geosmin elicited significantly stronger activation in the *moj*DA2 glomerulus of the cactophilic species *D. mojavensis*, and this glomerulus is twice as big as its homolog in other species (Figures 3, 4, and 5). Interestingly, despite its increased sensitivity, *D. mojavensis* flies are not repelled by the smell of geosmin (Figure 2). In the context of a desert species like *D. mojavensis*, an earthy smell could indicate a water source, which could explain why flies of this species are no longer aversed by the smell of geosmin. Future studies focusing on different behavioral aspects could shed light on the ecological relevance of geosmin in the cactophilic species.

scale was set to the strongest activated glomeruli of the four images selected for each species independently. The image of the response evoked by geosmin corresponds to a more dorsal focal plane to better visualize the DA2 glomerulus.
(B) Heatmap of the average responses in each species. ΔF/F was normalized (see STAR Methods), and the same scale was applied to all heatmaps to allow for comparison between species. The valence is indicated next to each odorant (green, attractive; white, neutral; red, aversive). E. 2-methyl butyrate, ethyl 2-methyl butyrate; E. 3-hydroxybutyrate, ethyl-hydroxybutyrate.
Odorants were tested at a $10^{-3}$ concentration, except for geosmin, which was tested at $10^{-4}$.
See also Figures S4 and S5.

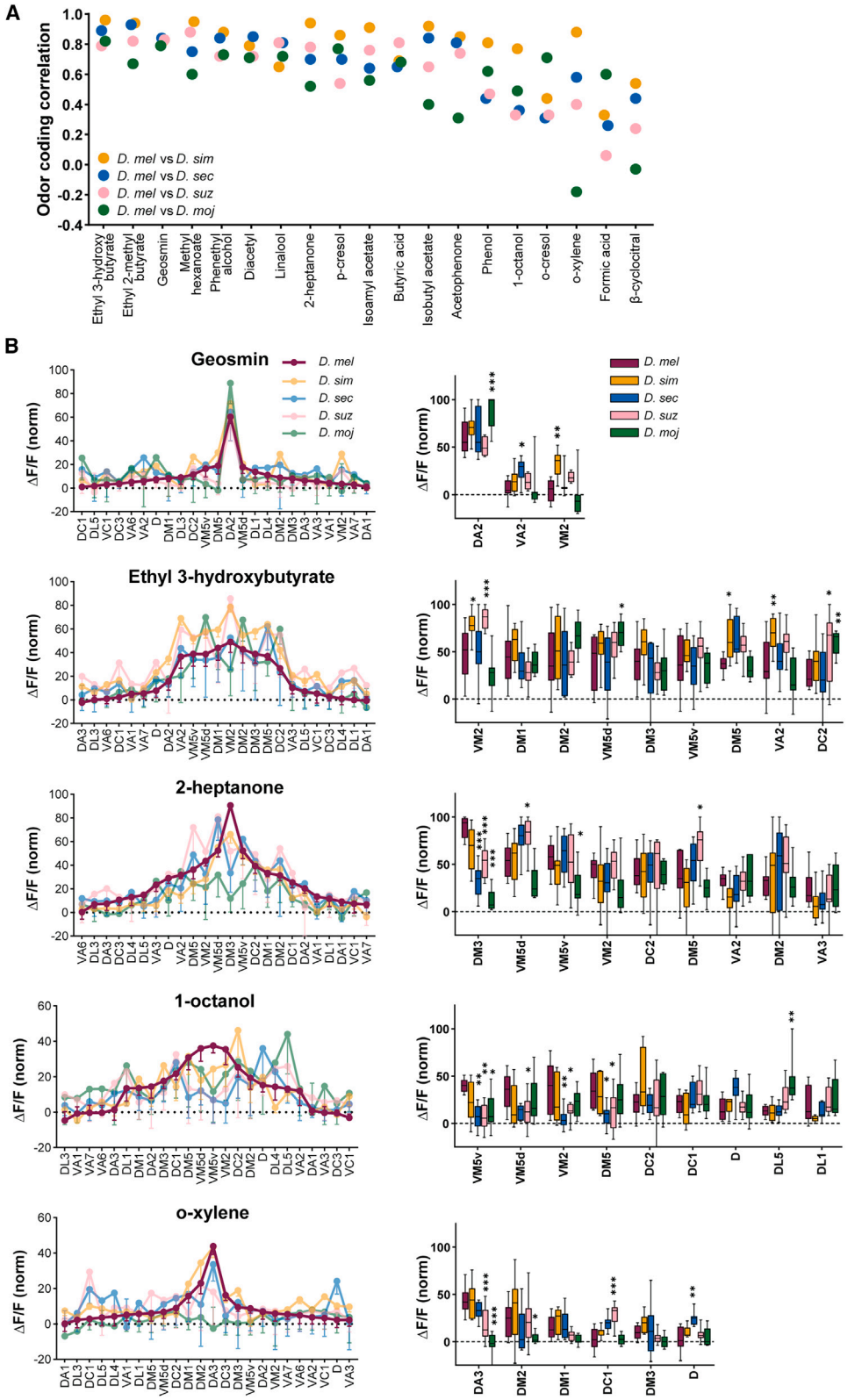


*(legend on next page)*

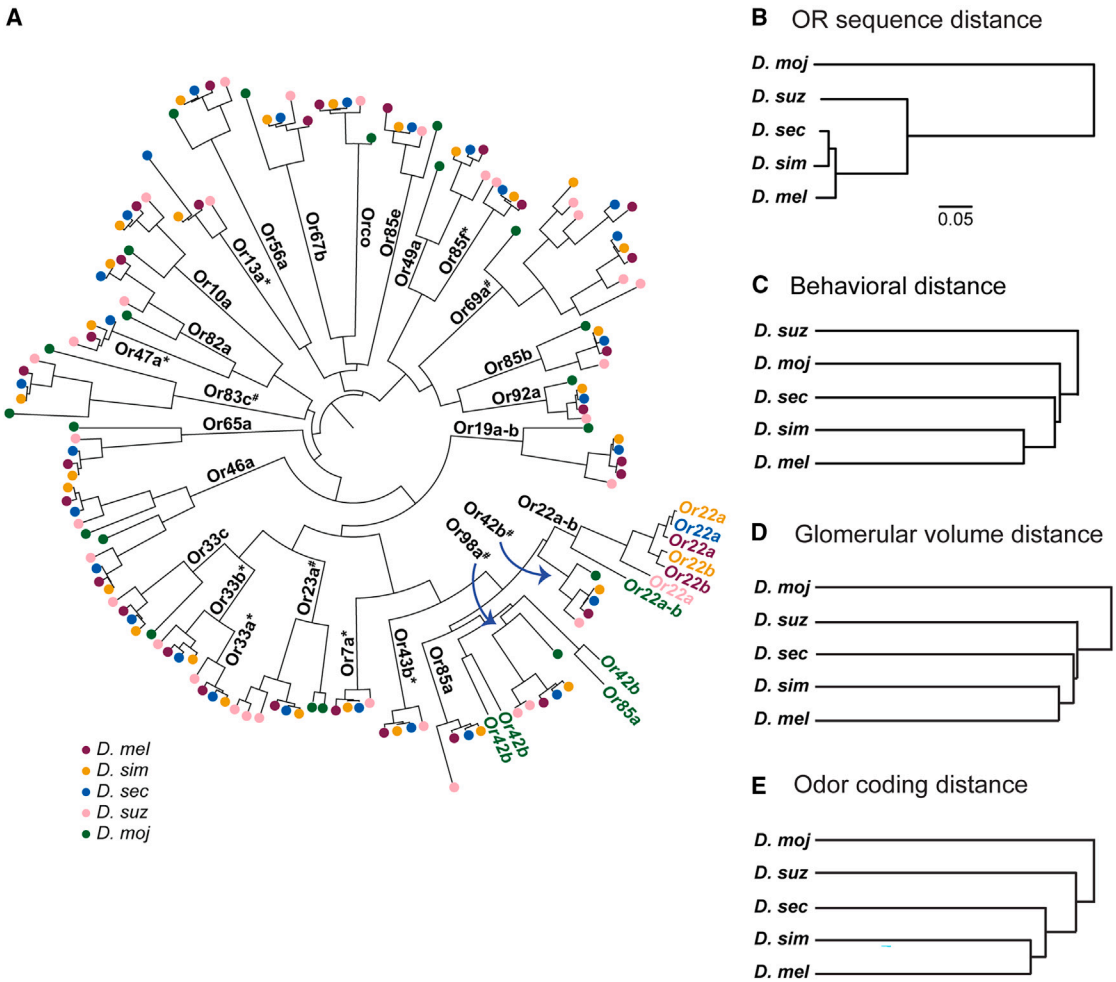


**Figure 6. Evolutionary distance and niche occupancy could explain the evolution of olfactory systems at multiple levels**

(A) Phylogenetic analysis of OR sequences. Only ORs putatively expressed in OSNs innervating the glomeruli analyzed in our study are included. The * and # indicate cases of OR loss or duplication, respectively. (Maximum-likelihood consensus tree, supported by 1,000 ultrafast bootstrap iterations; see STAR Methods for more details.)

(B) Phylogenetic analysis based only on the sequences of the ORs in (A) (maximum-likelihood consensus tree, supported by 500 bootstrap iterations; see STAR Methods for more details). Scale bars, 0.05 nucleotide substitutions per site.

(C–E) Hierarchical cluster analysis of behavioral responses (C), glomerular volume (D), and odor response patterns in the AL (E) for each species. (Euclidean distances, single linkage.)

See also Figure S6 and Table S4.

## Evolution of olfactory circuits

The peripheral olfactory system possesses multiple components that can undergo evolutionary changes and, as a consequence, alter the way in which related species detect an odorant. The most basic level is the ORs directly detecting the chemicals. Mutations altering receptor tuning, loss of receptors, and diversification of receptors via gene duplication have been characterized for some species.[29,34,53] In the present study, we found a negative correlation between the diversification of OR sequence and the conservation of odorant responses in the putatively corresponding glomeruli across species (Figure 7B). Although a detailed study of how specific OR mutations alter the receptor tuning was out of our scope, we believe our work paves the way for future work focusing on the genetic basis of odor tuning across species.

**Figure 5. Different degrees of odor coding conservation between species**

(A) Odor coding correlation between *D. melanogaster* and the other four species. Odorants are sorted from more conserved to less conserved coding patterns.

(B) Left: mean responses (ΔF/Fnorm) in all glomeruli for five representative odorants (mean ± SD, n = 6–14 brains). Right: mean responses for the most responsive glomeruli for each odorant (see STAR Methods). Mean responses of each species were compared with those of *D. melanogaster* (ANOVA followed by Dunnett's post hoc test, except for responses in VA2 for geosmin, DM5 for 2-heptanone, DL1 and DL5 for 1-octanol, and DM3 for o-xylene, which were compared via a non-parametric Kruskal-Wallis test due to a lack of normality of the data). Boxplots depict median responses, interquartile ranges, and maximum and minimum values.

See also Data S1.

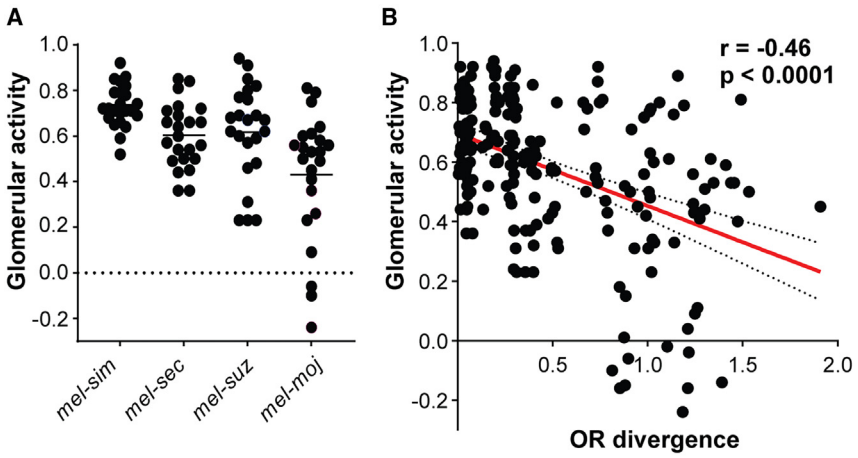


**Figure 7. Changes in OR sequence might be partially responsible for the change in odor coding**

(A) Correlation of glomerular activity between *D. melanogaster* and the other four species. Each dot represents the Pearson correlation value for each glomerular unit, considering the responses of all tested odorants.

(B) Negative correlation between glomerular tuning similarity and OR divergence (Dist_ORseq) between species.

Another mechanism susceptible to evolutionary change is the number of OSNs expressing specific receptors. A recent study from our group analyzed the distribution of large basiconic sensilla in the antenna of 20 species and found species with ab1, ab2, or ab3 bias, suggesting interspecies differences in the proportion of OSN numbers.[31] Increasing the number of certain OSNs can increase the sensitivity to certain chemicals. Moreover, given that most odorants are detected in a combinatorial manner, an increase in OSNs expressing certain receptors would exacerbate the importance of that channel in odor coding. Consistent with the increased sensitivity to methyl hexanoate, *D. sechellia* possesses more OSNs expressing Or22a.[29] In *D. melanogaster*, the number of OSNs per glomerulus correlates with glomerular volume.[54] Indeed, the increase in OSNs expressing Or22a, as well as those expressing Ir75b, in *D. sechellia* correlates with an enlarged volume of the targeted glomeruli (Figure 3B; Table S3; Prieto-Godino et al.[28]; Dekker et al.[36]). Another interesting case is that of the *D. suzukii* DA1 glomerulus. In *D. suzukii*, the cVA-responding glomerulus DA1 is strikingly reduced in volume due to a reduced number of trichoid sensilla harboring the Or67b receptor. This reduction of Or67b$^{+}$-OSNs could have driven or been the product of the loss of the sex pheromone cVA in this species, but in both cases, it highlights the importance of changes in OSN number as an evolutionary mechanism to modulate odor perception (Figure 3B; Dekker et al.[55]). Even more, changes in the number of certain OSN types have been reported even between subspecies of *D. mojavensis*.[36,56]

Here, we found several cases of enlargement and reduction of glomerular volume, among them the changes mentioned above in *D. sechellia* and *D. suzukii* glomeruli (Figure 3B; Table S3). Future experiments are required to study whether these glomerular volume changes result from a change in OSN numbers across species. It should be mentioned that the comparison of glomerular volume is based on the assumption that all glomeruli in the non-*melanogaster* species are correctly identified, something that would remain to be confirmed by tracing individual OSN types by backfilling techniques or transgenic lines for specific ORs in each species. Nonetheless, the fact that we found volume changes in those glomeruli where a change in the number of corresponding OSNs had been reported before,[28,29,31,37,55] gives us confidence that position and shape are good identifiers for homologous glomeruli.

In addition, it is worth mentioning that an increase in glomerular volume could, in principle, also be a result of changes in the synaptic arborizations without altering the number of OSNs. Furthermore, they could also result from increased inhibitory lateral interneurons that also arborize in the glomeruli. In the latter case, a larger glomerulus volume would suggest that the activity of the OSNs innervating that glomerulus is further inhibited and hence contributes less to the odor coding.

## Olfactory changes driving behavioral switch across species

In our behavioral screen, we found several odorants triggering opposite behaviors across species, suggesting that the same odorants can have different valences in related species (Figure 2). It is hypothesized that changes in the sequences of chemoreceptors alter chemical detection and are a driver of behavioral change between species. This could be the case in some species where the loss of attraction to certain chemicals correlates with changes in receptor tuning due to mutations in gustatory, ionotropic, or olfactory receptors.[28,29,57,58] Contrary to this hypothesis, we did not observe that odorants with a changed valence across species have a more dissimilar odor coding globally than those with a conserved valence (Figure S5A). Moreover, 2-heptanone, an odorant that elicits attraction in *D. melanogaster* but aversion in *D. simulans*, elicits indistinguishable response patterns at the OSN level analyzed here (Figure 5B).

It is noteworthy that our genetic tools did not allow us to record responses of OSNs expressing IRs, which could have a relevant role in the responses to specific host odorants, e.g., acid detection in *D. sechellia*. Although we cannot rule out the role of OSNs expressing IRs, several facts point to other mechanisms involved in changes in odor-guided behavior across species.

First, in *D. melanogaster*, responses to attractive and aversive odors are not clearly separated at the level of OSN terminals in the AL.[43] On the contrary, innate odor valence is first represented at the level of second-order neurons, i.e., PNs, in the AL and subsequently in higher brain structures, such as the lateral horn.[59,60]

Second, changes in other neuronal populations, such as local interneurons, projection neurons, or even further circuits comprising higher-order neurons, could be responsible for changes in the observed species-specific preference behavior. For example, in *D. melanogaster* larvae, the hunger state triggers a switch from attraction to aversion toward geranyl acetate by altering the balance between two neuronal pathways required

for opposing behavioral responses.[61] Also, the change from courtship promotion in *D. melanogaster* to courtship suppression in *D. simulans* by the sex pheromone 7,11-heptacosadiene is not due to changes in the odor detection at the periphery but to a differential propagation of the olfactory information onto upstream brain circuits controlling courtship behavior.[45]

Finally, our data suggest that the overall evolution of olfactory behaviors does not rely on changes at one processing level only. Although such single evolutionary changes have previously been shown to be important, the research has always focused on only one or two odorants, analyzed only pairs of species, or studied olfactory coding in a small subset of ORs or glomeruli.[14,28,29,31–38] On the contrary, our study demonstrates that when analyzing at a higher scale, changes in behavior are not always the consequence of evolutionary changes at one particular level.

To conclude, our results support a model where changes in the primary detection of odorants are not always required or necessarily the most important mechanism driving behavioral shifts. From our perspective, behavioral change across species is likely to be a complex evolutionary process that relies on changes at different levels.

## STAR★METHODS

Detailed methods are provided in the online version of this paper and include the following:

- KEY RESOURCES TABLE
- RESOURCE AVAILABILITY
  - Lead contact
  - Materials availability
  - Data and code availability
- EXPERIMENTAL MODEL AND SUBJECT DETAILS
  - Fly rearing and stocks
  - Generation of transgenic lines
- METHOD DETAILS
  - Chemical analysis and electrophysiology
  - Olfactory trap ssays
  - Immunofluorescence and antennal lobe reconstruction
  - Wide-field calcium imaging
  - Phylogenetic analysis
- QUANTIFICATION AND STATISTICAL ANALYSIS
  - Behavioral assays
  - Antennal lobe reconstructions
  - Calcium imaging analysis
  - Statistical analysis and figure preparation

## SUPPLEMENTAL INFORMATION

Supplemental information can be found online at https://doi.org/10.1016/j.cub.2023.09.039.

## ACKNOWLEDGMENTS

We thank Dr. Benjamin Prud'homme, Dr. David Stern, the Bloomington Stock Center, and the National *Drosophila* Species Stock Center for sharing fly stocks and plasmids. We also thank Veit Grabe, Angela Lehmann, Silke Trauheim, Roland Spieß, and Kerstin Weniger for their technical support, expertise, and guidance. We would like to thank Nicolás Pirez for his suggestions and comments on the manuscript. This research was funded by the Max Planck Society and an Alexander von Humboldt Foundation grant (to A.D.-C.). The artistic work is courtesy of D.G. (Sci-flies.com).

## AUTHOR CONTRIBUTIONS

A.D.-C. performed the behavioral experiments, chemical analysis, AL reconstructions, and functional imaging and analyzed all data generated here. A.D.-C. was co-supervised by S.S. and M.K. D.G. generated molecular reagents and transgenic lines in non-*melanogaster* species and performed the phylogenetical analysis. A.D.-C. carried out electrophysiology experiments with the assistance of I.W.K. A.D.-C., B.S.H., S.S., and M.K. conceived the project, and A.D.-C., S.S., and M.K. designed the experiments and interpreted the results. A.D.-C. prepared the figures and wrote the manuscript with input from the other authors.

## DECLARATION OF INTERESTS

The authors declare no competing interests.

## INCLUSION AND DIVERSITY

We support inclusive, diverse, and equitable conduct of research.

Received: May 11, 2023
Revised: August 2, 2023
Accepted: September 15, 2023
Published: October 6, 2023

## REFERENCES

1. Von Uexküll, J., and Kriszat, G. (1934). Streifzüge Durch die Umwelten von Tieren und Menschen Ein Bilderbuch unsichtbarer Welten (Springer).
2. Oteiza, P., and Baldwin, M.W. (2021). Evolution of sensory systems. Curr. Opin. Neurobiol. *71*, 52–59.
3. Couto, A., Wainwright, J.B., Morris, B.J., and Montgomery, S.H. (2020). Linking ecological specialisation to adaptations in butterfly brains and sensory systems. Curr. Opin. Insect Sci. *42*, 55–60.
4. Stevens, M. (2013). Sensory Ecology, Behaviour, and Evolution (Oxford University Press, Inc.). https://doi.org/10.1093/acprof:oso/9780199601776.001.0001.
5. Spoor, F., Bajpai, S., Hussain, S.T., Kumar, K., and Thewissen, J.G.M. (2002). Vestibular evidence for the evolution of aquatic behaviour in early cetaceans. Nature *417*, 163–166.
6. Wada-Katsumata, A., Silverman, J., and Schal, C. (2013). Changes in taste neurons support the emergence of an adaptive behavior in cockroaches. Science *340*, 972–975.
7. Auer, T.O., Shahandeh, M.P., and Benton, R. (2021). *Drosophila sechellia*: a genetic model for behavioral evolution and neuroecology. Annu. Rev. Genet. *55*, 527–554.
8. Karageorgi, M., Bräcker, L.B., Lebreton, S., Minervino, C., Cavey, M., Siju, K.P., Grunwald Kadow, I.C., Gompel, N., and Prud'homme, B. (2017). Evolution of multiple sensory systems drives novel egg-laying behavior in the fruit pest *Drosophila suzukii*. Curr. Biol. *27*, 847–853. https://doi.org/10.1016/j.cub.2017.01.055.
9. Dweck, H.K.M., Talross, G.J.S., Wang, W., and Carlson, J.R. (2021). Evolutionary shifts in taste coding in the fruit pest *Drosophila suzukii*. eLife *10*, 1–29.
10. Markow, T.A., and O'Grady, P. (2006). *Drosophila*: a Guide to Species Identification and Use (Elsevier), p. 259. https://doi.org/10.1017/CBO9781107415324.004.
11. Markow, T.A., and O'Grady, P. (2008). Reproductive ecology of *Drosophila*. Funct. Ecol. *22*, 747–759.
12. Becher, P.G., Flick, G., Rozpędowska, E., Schmidt, A., Hagman, A., Lebreton, S., Larsson, M.C., Hansson, B.S., Piškur, J., Witzgall, P., et al. (2012). Yeast, not fruit volatiles mediate *Drosophila melanogaster* attraction, oviposition and development. Funct. Ecol. *26*, 822–828.

13. Brummel, T., Ching, A., Seroude, L., Simon, A.F., and Benzer, S. (2004). *Drosophila* lifespan enhancement by exogenous bacteria. Proc. Natl. Acad. Sci. USA *101*, 12974–12979.

14. Linz, J., Baschwitz, A., Strutz, A., Dweck, H.K., Sachse, S., Hansson, B.S., and Stensmyr, M.C. (2013). Host plant-driven sensory specialization in Drosophila erecta. Proc. R. Soc. Lond. B *298*, 20130626.

15. Depetris-Chauvin, A., Galagovsky, D., and Grosjean, Y. (2015). Chemicals and chemoreceptors: ecologically relevant signals driving behavior in *Drosophila*. Front. Ecol. Evol. *3*, 41.

16. Mansourian, S., and Stensmyr, M.C. (2015). The chemical ecology of the fly. Curr. Opin. Neurobiol. *34*, 95–102.

17. Aranha, M.M., and Vasconcelos, M.L. (2018). Deciphering *Drosophila* female innate behaviors. Curr. Opin. Neurobiol. *52*, 139–148.

18. Gomez-Diaz, C., Martin, F., Garcia-Fernandez, J.M., and Alcorta, E. (2018). The two main olfactory receptor families in *Drosophila*, ORs and IRs: a comparative approach. Front. Cell. Neurosci. *12*, 253.

19. del Mármol, J., Yedlin, M.A., and Ruta, V. (2021). The structural basis of odorant recognition in insect olfactory receptors. Nature *597*, 126–131.

20. Grabe, V., and Sachse, S. (2018). Fundamental principles of the olfactory code. Biosystems. *164*, 94–101.

21. Wilson, R.I. (2013). Early olfactory processing in *Drosophila*: mechanisms and principles. Annu. Rev. Neurosci. *36*, 217–241.

22. Laissue, P.P., and Vosshall, L.B. (2008). The olfactory sensory map in *Drosophila*. In Brain Development in Drosophila melanogaster, G.M. Technau, ed. (Landes Bioscience and Springer Science), pp. 102–114.

23. Das Chakraborty, S., and Sachse, S. (2021). Olfactory processing in the lateral horn of *Drosophila*. Cell Tissue Res. *383*, 113–123.

24. Hayden, S., Bekaert, M., Crider, T.A., Mariani, S., Murphy, W.J., and Teeling, E.C. (2010). Ecological adaptation determines functional mammalian olfactory subgenomes. Genome Res. *20*, 1–9.

25. Hughes, G.M., Boston, E.S.M., Finarelli, J.A., Murphy, W.J., Higgins, D.G., and Teeling, E.C. (2018). The birth and death of olfactory receptor gene families in mammalian niche adaptation. Mol. Biol. Evol. *35*, 1390–1406.

26. Yohe, L.R., Fabbri, M., Hanson, M., and Bhullar, B.-A.S. (2020). Olfactory receptor gene evolution is unusually rapid across Tetrapoda and outpaces chemosensory phenotypic change. Curr. Zool. *66*, 505–514.

27. Goldman-Huertas, B., Mitchell, R.F., Lapoint, R.T., Faucher, C.P., Hildebrand, J.G., and Whiteman, N.K. (2015). Evolution of herbivory in Drosophilidae linked to loss of behaviors, antennal responses, odorant receptors, and ancestral diet. Proc. Natl. Acad. Sci. USA *112*, 3026–3031.

28. Prieto-Godino, L.L., Rytz, R., Cruchet, S., Bargeton, B., Abuin, L., Silbering, A.F., Ruta, V., Dal Peraro, M., and Benton, R. (2017). Evolution of acid-sensing olfactory circuits in Drosophilids. Neuron *93*, 661–676.e6.

29. Auer, T.O., Khallaf, M.A., Silbering, A.F., Zappia, G., Ellis, K., Álvarez-Ocaña, R., Arguello, J.R., Hansson, B.S., Jefferis, G.S.X.E., Caron, S.J.C., et al. (2020). Olfactory receptor and circuit evolution promote host specialization. Nature *579*, 402–408. https://doi.org/10.1038/s41586-020-2073-7.

30. Nozawa, M., and Nei, M. (2007). Evolutionary dynamics of olfactory receptor genes in *Drosophila* species. Proc. Natl. Acad. Sci. USA *104*, 7122–7127.

31. Zhao, Z., and McBride, C.S. (2020). Evolution of olfactory circuits in insects. J. Comp. Physiol. A Neuroethol. Sens. Neural Behav. Physiol. *206*, 353–367.

32. Anholt, R.R.H. (2020). Chemosensation and evolution of *Drosophila* host plant selection. iScience *23*, 100799.

33. Ramasamy, S., Ometto, L., Crava, C.M., Revadi, S., Kaur, R., Horner, D.S., Pisani, D., Dekker, T., Anfora, G., and Rota-Stabelli, O. (2016). The evolution of olfactory gene families in *Drosophila* and the genomic basis of chemical-ecological adaptation in *Drosophila suzukii*. Genome Biol. Evol. *8*, 2297–2311.

34. Hickner, P.V., Rivaldi, C.L., Johnson, C.M., Siddappaji, M., Raster, G.J., and Syed, Z. (2016). The making of a pest: insights from the evolution of chemosensory receptor families in a pestiferous and invasive fly, *Drosophila suzukii*. BMC Genomics *17*, 648.

35. Crowley-Gall, A., Date, P., Han, C., Rhodes, N., Andolfatto, P., Layne, J.E., and Rollmann, S.M. (2016). Population differences in olfaction accompany host shift in *Drosophila mojavensis*. Proc. Biol. Sci. *283*, 101–109.

36. Dekker, T., Ibba, I., Siju, K.P., Stensmyr, M.C., and Hansson, B.S. (2006). Olfactory shifts parallel superspecialism for toxic fruit in *Drosophila melanogaster* sibling, *D. sechellia*. Curr. Biol. *16*, 101–109.

37. Lebreton, S., Borrero-Echeverry, F., Gonzalez, F., Solum, M., Wallin, E.A., Hedenström, E., Hansson, B.S., Gustavsson, A.L., Bengtsson, M., Birgersson, G., et al. (2017). A *Drosophila* female pheromone elicits species-specific long-range attraction via an olfactory channel with dual specificity for sex and food. BMC Biol. *15*, 88.

38. Keesey, I.W., Zhang, J., Depetris-Chauvin, A., Obiero, G.F., Gupta, A., Gupta, N., Vogel, H., Knaden, M., and Hansson, B.S. (2022). Functional olfactory evolution in *Drosophila suzukii* and the subgenus Sophophora. iScience *25*, 104212.

39. Keesey, I.W., Knaden, M., and Hansson, B.S. (2015). Olfactory specialization in *Drosophila suzukii* supports an ecological shift in host preference from rotten to fresh Fruit. J. Chem. Ecol. *41*, 121–128.

40. Date, P., Crowley-Gall, A., Diefendorf, A.F., and Rollmann, S.M. (2017). Population differences in host plant preference and the importance of yeast and plant substrate to volatile composition. Ecol. Evol. *7*, 3815–3825.

41. Khallaf, M.A., Cui, R., Weißflog, J., Erdogmus, M., Svatoš, A., Dweck, H.K.M., Valenzano, D.R., Hansson, B.S., and Knaden, M. (2021). Large-scale characterization of sex pheromone communication systems in *Drosophila*. Nat. Commun. *12*, 4165.

42. Dweck, H.K.M., Ebrahim, S.A.M., Retzke, T., Grabe, V., Weißflog, J., Svatoš, A., Hansson, B.S., and Knaden, M. (2018). The olfactory logic behind fruit odor preferences in larval and adult *Drosophila*. Cell Rep. *23*, 2524–2531.

43. Knaden, M., Strutz, A., Ahsan, J., Sachse, S., and Hansson, B.S. (2012). Spatial representation of odorant valence in an insect brain. Cell Rep. *1*, 392–399.

44. Date, P., Dweck, H.K.M., Stensmyr, M.C., Shann, J., Hansson, B.S., and Rollmann, S.M. (2013). Divergence in olfactory host plant preference in *D. mojavensis* in response to cactus host use. PLoS One *8*, 1–10.

45. Seeholzer, L.F., Seppo, M., Stern, D.L., and Ruta, V. (2018). Evolution of a central neural circuit underlies *Drosophila* mate preferences. Nature *559*, 564–569.

46. Laissue, P.P., Reiter, C., Hiesinger, P.R., Halter, S., Fischbach, K.F., and Stocker, R.F. (1999). Three-dimensional reconstruction of the antennal lobe in *Drosophila melanogaster*. J. Comp. Neurol. *405*, 543–552.

47. Stockinger, P., Kvitsiani, D., Rotkopf, S., Tirián, L., and Dickson, B.J. (2005). Neural circuitry that governs *Drosophila* male courtship behavior. Cell *121*, 795–807.

48. Ibba, I., Angioy, A.M., Hansson, B.S., and Dekker, T. (2010). Macroglomeruli for fruit odors change blend preference in *Drosophila*. Naturwissenschaften *97*, 1059–1066.

49. Guo, S., and Kim, J. (2007). Molecular evolution of *Drosophila* odorant receptor genes. Mol. Biol. Evol. *24*, 1198–1207.

50. Shaw, K.H., Johnson, T.K., Anderson, A., De Bruyne, M., and Warr, C.G. (2019). Molecular and functional evolution at the Odorant Receptor Or22 locus in *Drosophila melanogaster*. Mol. Biol. Evol. *36*, 919–929.

51. Gao, H.-H., Zhai, Y., Chen, H., Wang, Y., Liu, Q., Hu, Q., Ren, F., and Yu, Y. (2018). Ecological niche difference associated with varied ethanol tolerance between *Drosophila suzukii* and *Drosophila melanogaster* (Diptera: Drosophilidae). Fla. Entomol. *101*, 498–504.

52. Stensmyr, M.C., Dweck, H.K., Farhan, A., Ibba, I., Strutz, A., Mukunda, L., Linz, J., Grabe, V., Steck, K., Lavista-Llanos, S., et al. (2012). A conserved dedicated olfactory circuit for detecting harmful microbes in *Drosophila*. Cell *151*, 1345–1357.

53. Prieto-Godino, L.L., Rytz, R., Bargeton, B., Abuin, L., Arguello, J.R., Peraro, M.D., and Benton, R. (2016). Olfactory receptor pseudo-pseudogenes. Nature *539*, 93–97.

54. Grabe, V., Baschwitz, A., Dweck, H.K.M., Lavista-Llanos, S., Hansson, B.S., and Sachse, S. (2016). Elucidating the neuronal architecture of olfactory glomeruli in the *Drosophila* antennal lobe. Cell Rep. *16*, 3401–3413.

55. Dekker, T., Revadi, S., Mansourian, S., Ramasamy, S., Lebreton, S., Becher, P.G., Angeli, S., Rota-Stabelli, O., and Anfora, G. (2015). Loss of *Drosophila* pheromone reverses its role in sexual communication in *Drosophila suzukii*. Proc. Biol. Sci. *282*, 20143018.

56. Khallaf, M.A., Auer, T.O., Grabe, V., Depetris-Chauvin, A., Ammagarahalli, B., Zhang, D.D., Lavista-Llanos, S., Kaftan, F., Weißflog, J., Matzkin, L.M., et al. (2020). Mate discrimination among subspecies through a conserved olfactory pathway. Sci. Adv. *6*, eaba5279.

57. Cande, J., Prud'homme, B., and Gompel, N. (2013). Smells like evolution: the role of chemoreceptor evolution in behavioral change. Curr. Opin. Neurobiol. *23*, 152–158.

58. Wisotsky, Z., Medina, A., Freeman, E., and Dahanukar, A. (2011). Evolutionary differences in food preference rely on Gr64e, a receptor for glycerol. Nat. Neurosci. *14*, 1534–1541.

59. Strutz, A., Soelter, J., Baschwitz, A., Farhan, A., Grabe, V., Rybak, J., Knaden, M., Schmuker, M., Hansson, B.S., and Sachse, S. (2014). Decoding odor quality and intensity in the *Drosophila* brain. eLife *3*, e04147.

60. Das Chakraborty, S., Chang, H., Hansson, B.S., and Sachse, S. (2022). Higher-order olfactory neurons in the lateral horn supports odor valence and odor identity coding in *Drosophila*. eLife *11*, e74637.

61. Vogt, K., Zimmerman, D.M., Schlichting, M., Hernandez-Nunez, L., Qin, S., Malacon, K., Rosbash, M., Pehlevan, C., Cardona, A., and Samuel, A.D.T. (2021). Internal state configures olfactory behavior and early sensory processing in *Drosophila* larvae. Sci. Adv. *7*, 1–11.

62. Tamura, K., Stecher, G., and Kumar, S. (2021). MEGA11: molecular evolutionary genetics analysis, version 11. Mol. Biol. Evol. *38*, 3022–3027.

63. Nguyen, L.T., Schmidt, H.A., Von Haeseler, A., and Minh, B.Q. (2015). IQ-TREE: A fast and effective stochastic algorithm for estimating maximum-likelihood phylogenies. Mol. Biol. Evol. *32*, 268–274.

64. Edler, D., Klein, J., Antonelli, A., and Silvestro, D. (2021). raxmlGUI 2.0: A graphical interface and toolkit for phylogenetic analyses using RAxML. Methods Ecol. Evol. *12*, 373–377.

65. Grabe, V., Strutz, A., Baschwitz, A., Hansson, B.S., and Sachse, S. (2015). A digital in vivo 3D atlas of the antennal lobe of Drosophila melanogaster. The Journal of Comparative Neurology *523*, 530–544.

66. Rubin, G.M., and Spradling, A.C. (2021). Genetic transformation of *Drosophila* with transposable element vectors. Science *218*, 348–353.

67. Strutz, A., Völler, T., Riemensperger, T., Fiala, A., and Sachse, S. (2012). Calcium imaging of neural activity in the olfactory system of *Drosophila*. In Genetically Encoded Functional Indicators, J.-R. Martin, ed. (Humana Press), pp. 43–70. https://doi.org/10.1007/978-1-62703-014-4_3.

68. Sayers, E.W., Karsch-Mizrachi, I., Clark, K., Lipman, D.J., Ostell, J., and Sayers, E.W. (2022). GenBank. Nucleic Acids Res. *50*, 92–107.

69. Kalyaanamoorthy, S., Minh, B.Q., Wong, T.K.F., Von Haeseler, A., and Jermiin, L.S. (2017). ModelFinder: fast model selection for accurate phylogenetic estimates. Nat. Methods *14*, 587–589.

70. Hoang, D.T., Chernomor, O., Von Haeseler, A., Minh, B.Q., and Vinh, L.S. (2018). UFBoot2: improving the ultrafast bootstrap approximation. Mol. Biol. Evol. *35*, 518–522.

## STAR★METHODS

### KEY RESOURCES TABLE

| REAGENT or RESOURCE | SOURCE | IDENTIFIER |
|---|---|---|
| Antibodies | | |
| Rabbit anti-GFP | Thermo Fisher Scientific | Cat#A11122; RRID: AB_221569 |
| Mouse monoclonal NC82 | Developmental Studies Hybridoma Bank | Cat#A1Z7V1; RRID: 35977 |
| Goat anti-mouse Alexa Fluor 633 | Thermo Fisher Scientific | Cat#A21052; RRID: AB_2535719 |
| Goat anti-rabbit Alexa Fluor 488 | Thermo Fisher Scientific | Cat#A32731; RRID: AB_143165 |
| Normal Goat Serum | Merck | Cat# S26-100ML |
| Chemicals, peptides, and recombinant proteins | | |
| Vectashield Antifade Mounting Media | Vector Laboratories | Cat#H-1000-10 |
| Paraformaldehyde, granulated | Carl Roth GmBH | Cat#0335.2 |
| Hexane (CAS 110-54-3) | Carl Roth GmBH | Cat#KK48.1 |
| Mineral oil (CAS 8042-47-5) | VWR Life Science | Cat#J217 |
| Triton X (CAS 9036-19-5) | Sigma-Aldrich | Cat#X100 |
| Agar-agar | Carl Roth GmBH | Cat#5210 |
| Nipagin | Sigma-Aldrich | Cat#H5501 |
| Propionic acid (CAS 79-09-4) | Carl Roth GmBH | Cat#6026 |
| EXPAND Long Template PCR System Roche | Sigma-Aldrich | Cat#11681834001 |
| Gateway LR Clonase II Enzyme mix | Invitrogen | Cat#11791020 |
| SbfI-HF restriction enzyme | New England Biolabs | Cat#R3642S |
| BmtI restriction enzyme | New England Biolabs | Cat#R0658S |
| AvrII restriction enzyme | New England Biolabs | Cat#R0174S |
| See Table S5 for chemicals used as odorants. | N/A | N/A |
| Critical commercial assays | | |
| QIAGEN DNAeasy Blood and Tissue Kit | Qiagen | Cat#69504 |
| TOPO XL-2 Complete PCR Cloning Kit | Invitrogen | Cat#K8050-10 |
| pCR8/GW/TOPO TA Cloning Kit | Invitrogen | Cat#K250020 |
| Deposited data | | |
| *D. simulans*: reference genome sequence | NIH - NCBI | ASM438218v1 |
| *D. sechellia*: reference genome sequence | NIH - NCBI | ASM438219v1 |
| *D. suzukii*: reference genome sequence | NIH - NCBI | Dsuzukii.v01 |
| *D. mojavensis wrigleyi*: reference genome sequence | NIH - NCBI | dmoj_caf1 |
| Experimental models: Organisms/strains | | |
| *D. melanogaster*: Wild-type Canton S | Bloomington Drosophila Stock Center | BDSC 64349 |
| *D. melanogaster*: *Orco* -GAL4 | Andre Fiala lab | N/A |
| *D. melanogaster*: UAS-GCaMP6f | Bloomington Drosophila Stock Center | BDSC 42747 |
| *D. simulans*: Wild-type | National Drosophila Species Stock Center | NDSSC 14021-0251.01 |
| *D. simulans*: *white[501]* | National Drosophila Species Stock Center | NDSSC (14021-0251.011) |
| *D. simulans*: *Orco* -GAL4 | This paper | N/A |
| *D. simulans*: UAS-GCaMP6s | Stern lab | Seeholzer et al.[45] |
| *D. sechellia*: Wild-type | National Drosophila Species Stock Center | NDSSC (14021-0248.07) |
| *D. sechellia*: *Orco* -GAL4 | This paper | N/A |
| *D. sechellia*: UAS-GCaMP6f | This paper | N/A |
| *D. suzukii*: Wild-type | National Drosophila Species Stock Center | NDSSC (14023-0311.01) |
| *D. suzukii*: *Orco* -GAL4 | This paper | N/A |
| *D. suzukii*: UAS-GCaMP6f | This paper | N/A |

(*Continued on next page*)

| *Continued* | | |
|---|---|---|
| REAGENT or RESOURCE | SOURCE | IDENTIFIER |
| *D. mojavensis wrigleyi*: Wild-type | National Drosophila Species Stock Center | NDSSC (15081-1352.30) |
| *D. mojavensis wrigleyi*: *Orco* -GAL4 | This paper | N/A |
| *D. mojavensis wrigleyi*: UAS-GCaMP6f | This paper | N/A |
| Oligonucleotides | | |
| See Table S6 | N/A | N/A |
| Recombinant DNA | | |
| pBac-3XP3GFP_hspGa4sv40attB | Prud'homme lab | N/A |
| pBac-3xP3-DsRed-7xUAS-hsp-GWR1R2-SV40 | Prud'homme lab | N/A |
| pBac-Helper plasmid | Prud'homme lab | N/A |
| pGP-CMV-GCaMP6f | Douglas Kim lab | RRID: Addgene_40755 |
| pBac-20XUAS-GCaMP6f,3XP3::dsRed | Stern lab | N/A |
| Software and algorithms | | |
| MSD ChemStation F.01.03.2357 | Agilent Technologies | N/A |
| NIST Mass Spectral Search Program 2.2 | Scientific Instrument Services | N/A |
| AutoSpike32 (v3.7) | Syntech | N/A |
| AMIRA version 5.6.0 | FEI Visualization Sciences Group | N/A |
| Adobe Acrobat X Pro (Adobe Systems, San Jose, CA). | Adobe Systems Incorporated | N/A |
| FIJI (ImageJ 1.52p) | National Institutes of Health, USA | http://imagej.nih.gov/ij |
| Molecular Evolutionary Genetics Analysis (MEGA) software version 11 | https://www.megasoftware.net/ | Tamura et al.[62] |
| iqTree v1.6.12 | http://www.iqtree.org/ | Nguyen et al.[63] |
| FigTree v1.4.4 | http://tree.bio.ed.ac.uk/software/figtree/ | N/A |
| Geneious Prime v11.0.18+10 | Biomatters Ltd. www.geneious.com | N/A |
| RAxMLGUI v2.0.10 | https://antonellilab.github.io/raxmlGUI/ | Edler et al.[64] |
| InfoStat package version 2009 | Grupo InfoStat | Universidad Nacional de Cordoba, Argentina |
| GraphPad Prism 9.0.2 | GraphPad Software | N/A |
| Microsoft Excel 2016 | Microsoft Corporation | N/A |
| Adobe Photoshop CS5 | Adobe Systems Incorporated | N/A |
| Adobe Illustrator CS5 | Adobe Systems Incorporated | N/A |

## RESOURCE AVAILABILITY

### Lead contact

Further information and requests for resources should be directed to and will be fulfilled by the lead contact, Markus Knaden (mknaden@ice.mpg.de).

### Materials availability

Further information and requests for resources and reagents should be directed to and will be fulfilled by the lead contact.

### Data and code availability

- All raw data supporting the findings of this study are available through Edmond, the Open Access Data Repository of the Max Planck Society at https://doi.org/10.17617/3.U5HMGE (raw data) and https://doi.org/10.17617/3.ZWVXDX (3d-reconstructions of atlases).
- This study did not generate unique "standardized datatypes" or original code.
- Any additional information about the data reported in this paper is available from the lead contact upon request.

## EXPERIMENTAL MODEL AND SUBJECT DETAILS

### Fly rearing and stocks

Flies were raised at 25 °C under 12:12 h light: dark cycles and 70% humidity, except for *D. suzukii* strains that were grown and maintained at 22 °C. All stocks were maintained in a standard cornmeal agar medium (cornmeal (10% m/v), agar (0.4% m/v), golden syrup (12 % m/v), yeast (1% m/v), propionic acid (0.25% v/v), nipagin 30% (0.3% v/v)) with the following additives to optimize culture in other species: smashed blueberries for the *D. suzukii* stocks, and for *D. sechellia* strains a thin layer of formula 4-24 instant *Drosophila* medium, blue (Carolina Biological Supply) soaked in noni juice (nu3 and Raab Vital food).

A complete list of the stocks and the stock numbers can be found in the key resources table.

### Generation of transgenic lines

#### *Molecular cloning*

*Orco*-Gal4 stocks were generated by cloning the DNA upstream from the *Orco* gene in each species, where the putative regulatory region was expected to be located, based on the existing *D. melanogaster* stocks. Genomic DNA was obtained from three adult flies using a QIAGEN DNAeasy Blood and Tissue Kit and later used as a template for PCR.

For *D. simulans*, a 7880 bp region upstream from the putative transcription start site was cloned. For *D. sechellia* and *D. mojavensis*, we cloned a 4413 bp and 4397 bp region upstream from the putative translation initiation site, respectively. For this, primers were designed based on publicly available reference genome sequences (*D. simulans* ASM438218v1, *D. mojavensis wrigleyi* dmoj_caf1, *D. sechellia* ASM438219v1, and *D. suzukii* Dsuzukii.v01). For *D. suzukii*, the site furthest from the gene fell on a gap in the publicly available sequence. To overcome this issue, a 9kb DNA fragment upstream from the gene was cloned using primers suzOrco1_F and suzOrco1_R and a touch-up PCR protocol. The unknown sequence of the central portion of this fragment was sequenced, and new primers with SbfI and BmtI restriction enzyme sites were designed to clone a 5095 bp region upstream from the putative translation initiation of Orco. A list of primers can be found in Table S6 named simOrco1, secOrco1, suzOrco1, suzOrco1_seq, and mojOrco1.

Fragments were cloned using EXPAND Long Template PCR System (Sigma-Aldrich) into TOPO XL-2 entry plasmids (Invitrogen) and further amplified using the same primers with the same binding region and added restrictions enzyme sites (SbfI and BmtI enzymes for *D. simulans*, *D. suzukii*, and *D. mojavensis*, and SbfI and AvrII enzymes for *D. sechellia*). Fragments were cloned into pbac-3XP3GFP_hspGa4sv40attB plasmid (a gift from Benjamin Prud'homme). Primers, i.e., simBmtI, simSbfI_R, secSbfI_F, secAvrII_R, suzSbfI_F, suzBmtI_R, mojBmtI_F, and mojSbfI_R, are listed in Table S6.

UAS-GCaMP6f stocks for *D. sechellia* and *D. mojavensis* were generated by cloning the GCaMP6f gene from the plasmid pGP-CMV-GCaMP6f (a gift from Douglas Kim & GENIE Project), cloned it into pCR8/GW/TOPO (Invitrogen), and later subcloned it into pBac-3xP3-DsRed-7xUAS-hsp-GWR1R2-SV40 (a gift from Benjamin Prud'homme) using the Gateway L-R recombinase (Invitrogen). *D. suzukii* UAS-GCaMP6f stock was directly produced via injection of pBac-20XUAS-GCaMP6f,3XP3::dsRed (a gift from David Stern).

#### Drosophila *microinjections*

Transgenic *D. simulans*, *D. sechellia*, *D. suzukii*, and *D. mojavensis wrigleyi* flies were produced through embryo microinjection.[62]

Each species was made to oviposit on agar plates with a specific composition tailored to their species' oviposition preferences to collect embryos. *D. simulans* plates consisted of 1.5% agar-agar and 3% sucrose; for *D. sechellia*, 1.5% agar-agar, 5% noni juice, and 5% agave syrup, plus a 1 $cm^2$ Whatmann paper imbibed in noni juice was stuck vertically in the center of the oviposition surface; for *D. suzukii*, the plates contained 3% agar-agar, 10% blueberry juice, and 3% strawberry syrup; and for *D. mojavensis*, 0.5% agar-agar, 10% prickly pear juice, and 5% agave syrup. In addition, oviposition plates for *D. simulans*, *D. sechellia*, and *D. mojavensis* were supplemented with a paste made from live granulated baker's yeast, and *D. suzukii*'s plates were supplemented with a paste consisting of dead baker's yeast mixed with potato starch and strawberry syrup.

Embryos were injected with a mix of injection buffer (5 mM KCl, 0.5 mM $NaH_2PO_4$ pH 7.8), pBac plasmid DNA (157.5 ng/ul), pBac-Helper plasmid DNA (78.75 ng/ul), and filtered food coloring, with the help of a microinjector (Narishige IM 300) fitted with an injection needle. Needles were made from borosilicate capillaries with filament (1.0 mm O.D., 0.5 mm I.D.; Sutter Instrument Co.) using a Flaming/Brown micropipette puller (Sutter Instrument Co. Model P-97).

## METHOD DETAILS

### Chemical analysis and electrophysiology

#### *Chemicals*

All synthetic odorants were purchased from commercial sources and were of the highest purity available. A list of chemicals used during this study is provided in Table S5. Odorants were diluted in hexane for chemical analysis or in mineral oil for behavioral and calcium imaging experiments, except for formic acid and γ-butyrolactone which were diluted in water supplemented with 0.1% of Triton X and methyl caprate diluted in dichloromethane according to solubility requirements.

#### *Chemical analysis*

Headspace volatiles were collected from commercial kiwi and cactus stems (*Opuntia ficus indica*) and in-house cultured noni fruit. Fresh samples were cut, placed in capped 500 ml glass bottles (FisherBrand) and maintained at room temperature. Headspaces

were collected at 10 days (noni fruit), 2, 6, and 8 weeks (cacti), or at two time points with visual differences in the fermentation stage (kiwi). Different fermentation stages of cacti and kiwi were further tested in behavioral assays (see below) to select the stage that elicits strong attraction in those species that have been previously described to be attracted to that plant (*D. mojavensis* for cactus, and *D. melanogaster*, *D. simulans*, and *D. suzukii* for kiwi). Headspaces were collected for 24 h using a push-pull system with a Super-Q filter (50 mg, www.volatilecollectiontrap.com) and eluted with 600 μl hexane. Headspace odor collections were analyzed by GC-MS using an HP5 UI column (19091S-433UI, Agilent Technologies, http://www.agilent.com) for kiwi and cactus samples and an HP-INNOWax column (Agilent 19091N-133UI) for noni samples for better identification of non-polar and polar components, respectively. Samples were injected at an initial oven temperature of 40 °C, held for 2 min, and increased gradually (15 °C $min^{-1}$) to 250 °C and held for 5 min. The mass spectrometry transfer line was held at 280 °C, the mass spectrometry source at 230 °C, and the mass spectrometry quad at 150 °C. Mass spectra were taken in EI-mode (70 eV) in a 33–350 m/z range. All chromatograms were analyzed using MSD ChemStation F.01.03.2357 software, and chemicals were identified using the NIST library (NIST Mass Spectral Search Program 2.2) and matched to the standards of the Max Planck Institute for Chemical Ecology library.

The concentration of each identified volatile was estimated by comparing the area under the peak in GC-MS runs with those of standards of known concentration. We then calculated the total content (%) of acids, esters, ketones, terpenes, alcohols, alkanes/alkenes, benzene derivatives, and other chemical groups in each fruit sample.

#### *Electroantennograms (EAD)*

Identification of antennal responsive odorants was conducted via GC-EAD, using the following stages: 2$^{nd}$ stage fermentation of kiwi, 10-day fermentation noni, and 6-weeks fermentation cactus. Young (2-8 days old) adult flies were immobilized in pipette tips and a glass electrode filled with Ringer solution ((NaCl: 130 mM, KCl: 5 mM, MgCl2:2 mM, CaCl2: 2 mM, Sucrose: 36 mM, HEPES-NaOH (pH 7.3): 5 mM) contacted one of the antennae. A second glass electrode was placed in contact with the eye to serve as a reference electrode.

For GC stimulation, 1 μl of headspace odor collection was injected onto a DB5 column (Agilent Technologies), fitted in an Agilent 6890 GC, equipped with a four-arm effluent splitter (Gerstel, www.gerstel.com), and operated with the same stimulation protocol than for the GC-MS analysis described above. One arm was connected with the GC's flame ionization detector (FID); the other arm was introduced into a humidified air stream (200 ml min-1) and directed toward the antennae of a mounted immobilized fly. No evident differences were observed between sexes. Signals from the antenna and FID were recorded simultaneously. The EAD signal was pre-amplified (10X), digitally converted, visualized, recorded, and later analyzed using AutoSpike software, version 3.7 (Syntech).

All identified responsive odorants were further confirmed by EAD with purchased chemical standards at the concentration that flies received in the GC-EAD configuration following the same procedure explained above in the Chemical analysis section. In addition, all chemicals identified by GC-MS in the cacti sample were tested individually for their EAD responses using chemical standards to maximize the identification of ecologically relevant odorants for each species. An odorant was considered to elicit a response when an EAD signal was observed in more than 50% of the cases tested with purchased chemical standards.

### Olfactory trap ssays

Mated females (7 days old for all species and 8 days old for *D. mojavensis* due to later reproductive development in this species) were starved (18-24 h) in groups of 30 and tested the following morning. The exact conditions of the behavioral assays were set independently for each species to optimize the fly' participation in the assay (i.e., increased the number of flies that chose one of the traps) and maximize odor responses, taking into consideration the specificities of each species. Briefly, the experiment arena consisted of a transparent plastic container (length, 10 cm; width, 8 cm; height, 10 cm) with 10 ventilation holes containing two traps (odor and solvent traps) made from small plastic vials (20 ml specimen container, VWR Collection) with a cut pipette tip inserted or a red-paper cone as an entrance, for *D. melanogaster* or non-*melanogaster* species respectively. To prevent dehydration, a small cotton ball soaked with distilled water was placed inside each test box. For olfactory trap assays, headspace collections were diluted at 1:5 (kiwi), 1:10 (cactus), or 1:100 (noni) in mineral oil. Test traps contained 400 μl (or 1 ml for *D. mojavensis*) of the solvent or the odorant/headspace collection diluted in the solvent. Single odorants were tested at a $10^{-3}$ concentration unless indicated otherwise. *D. sechellia* flies show a non-specific attraction towards most odorants after starvation. To avoid this, we added 5 μl of noni juice to both traps.

Experiments were carried out in a climate chamber (25 °C, 70% humidity, 12:12 h light: dark cycles), and the number of flies in each trap and outside the traps was counted after 24 h or 48 h for the case of *D. mojavensis*.

### Immunofluorescence and antennal lobe reconstruction

Adult flies' (2-8 days old) heads were fixed with 4% formaldehyde in 100 mM phosphate buffer pH 7.5 for 10 min. Brains were dissected and fixed for an additional 20 min at room temperature. Brains were rinsed 3x15 min in PBS with 0.3% Triton X-100 (PT), followed by incubation with primary antibodies in 4% normal goat serum (NGS) in PT (48 h at 4 C). Primary antibodies used were mouse monoclonal NC82 antibody (1:30) and rabbit anti-GFP (1:500). Samples were washed 4x20 min in PT, incubated overnight with secondary antibodies in NGS-PT, rinsed 4x20min in PT, and mounted in Vectashield. Secondary antibodies used were Alexa633-conjugated anti-mouse in (1:250) and Alexa488-conjugated anti-rabbit (1:250). Images were acquired with a Zeiss 710 NLO Confocal microscope using a 40x or 63x water immersion objectives.

Reconstruction of whole antennal lobes from *wt* female adult flies and individual glomeruli (3-6 antennal lobe specimens for each species) was performed manually using the segmentation software AMIRA version 5.6 (FEI Visualization Sciences Group). Additionally, 3-6 males for each species were dissected, and the sex-relevant glomeruli were reconstructed (DA1, VA1d, VA1v, and VL2a), and one female brain of Orco>GcaMP was reconstructed for each species to identify $Orco^+$ OSNs. Glomeruli was identified in non-melanogaster species by relative position in the antennal lobe as it was originally done in *D. melanogaster*. By comparing the reconstructed images of the different species to the map of *D. melanogaster* we have given the same name to glomerular structures with the same positioning and shape. This was further supported by our physiological data from $Ca^{2+}$ imaging recordings.

The ratio of antennal lobe over whole brain volume was calculated in another set of NC82 immunostained brains (6-9 female brains for each species).

A 3D PDF of the antennal lobe atlas for the five species was performed following the described procedure (Grabe et al.[65]). Reconstructed surfaces from AMIRA were imported in FIJI 3D viewer and transformed into universal 3d format (.u3d). Final adjustments of visualization parameters were done in Adobe Acrobat X Pro (Adobe Systems, San Jose, CA).

## Wide-field calcium imaging

### *Sample preparation*

Young (3-8 days old) Orco>GCaMP female flies (n = 6-14) were prepared for optical imaging as described before.[63] Briefly, flies were anesthetized on ice and mounted onto a custom-made Plexiglas stage with a copper plate (Athene Grids, Plano). A needle stabilized the proboscis, the head was glued to the stage using Protemp II (3M ESPE), and the antennae were pulled forward by a fine metal wire. Once immobilized, a plastic coverslip with a round window was placed on top of the fly head. A two-component silicon (World Precision Instruments) covered the surroundings of the round window to prevent the leaking of the Ringer solution ((NaCl: 130 mM, KCl: 5 mM, MgCl2:2 mM, CaCl2: 2 mM, Sucrose: 36 mM, HEPES-NaOH (pH 7.3): 5 mM)) onto the antennae. A small window was cut under Ringer solution in the fly head between the eyes and the ocelli. Finally, we removed the fat, trachea, and air sacs to better expose the antennal lobe and reduce light scattering.

We performed calcium imaging experiments using a wide field TillPhotonics imaging setup (TILL imago, http://www.till-photonics.com) equipped with a CCD camera (PCO imaging, http://www.pco.de) mounted on a fluorescence microscope (BX51WI, http://www.olympus.com) with a 20x water immersion objective (NA 0.95, XLUM Plan FI, http://www.olympus.com). Prior to odor exposure, a high-resolution Z stack covering the whole AL volume was performed to help with glomeruli identification. Samples were excited at 475 nm as described previously,[43] and the order of odor stimulation was randomized. We chose a single plane where we could reliably identify 24 $Orco^+$ glomeruli.

### *Odorant application*

10 μl of odorants at $10^{-3}$ (or $10^{-4}$ and $10^{-2}$ in the case of geosmin and diagnostic odorants, respectively) diluted in mineral oil were pipetted on a filter paper placed inside a glass Pasteur pipette. Odorants were applied with the help of a stimulus controller (Stimulus Controller CS-55; Syntech). A custom-made metal stage holding a stainless-steel tube directed a continuous airflow (1 L/min) and pulses of odorant (0.5 L/min) toward the fly's antennae. Odor stimuli were injected into the airstream after 2 s for a duration of 2 s. The recording frequency during imaging was 4 Hz with 40 frames (i.e., 10 s) in total.

In addition to the 19 odorants analyzed in this study, we screened a set of diagnostic odorants with defined activation patterns to facilitate glomerular identification (*i.e.*, DL5, benzaldehyde; DC2, 1-octen-3-ol, and for *D. mojavensis* glomeruli *moj*DM2 and *moj*VL5v, hexyl acetate; *moj*DM4 and *moj*VA2, dimethyl disulfide; *moj*DM1 and *moj*DM5, isopropyl benzoate).

Odorants were applied using a randomized order with at least a 1 min intra-stimulation interval to avoid habituation or interference in the odor responses.

## Phylogenetic analysis

Available OR sequences from *D. melanogaster*, *D. simulans*, *D. sechellia*, *D. suzukii*, and *D. mojavensis wrigleyi*[30,35] were updated, and missing sequences were completed by performing a Basic Local Alignment Search Tool (BLAST) analysis of all the sequences against the most current reference sequences available from the National Center for Biotechnology Information (NCBI[64]).

OR sequence codons were aligned via a Multiple Sequence Comparison by Log- Expectation (MUSCLE) using Molecular Evolutionary Genetics Analysis (MEGA) software version 11.[66] For the alignment, gaps were eliminated, and stop codons in the middle of some sequences, which were a product of their inferred nature, were ignored. For the phylogenetic analysis of the complete genome of 21 selected *Drosophila* species, coding sequences were obtained, processed, and aligned as described in Khallaf et al.[41] In both cases, we determined the best selection model from the alignments[67] and inferred the maximum-likelihood trees[68] using IQ-TREE software, obtaining branch supports from 1000 iterations with its ultrafast bootstrap.[69]

Evolutionary distances within each group of orthologues were calculated using the above-mentioned MEGA software. First, we performed a Multiple Sequence Comparison by Log- Expectation (MUSCLE) alignment of the codons of each individual group of putative orthologues. We then determined the best appropriate selection model and computed the pairwise distance accordingly using a 500-iteration bootstrap method to estimate the variance of the estimated distances.

For the phylogenetic analysis of the five species used in this study based only on the sequences of the ORs that are putatively expressed in OSNs innervating the glomeruli analyzed in our study, the sequences of each gene for each species were concatenated

using Geneious Prime (v2023.1.2, Biomatters Ltd.). An alignment was produced using Molecular Evolutionary Genetics Analysis (MEGA) software version 11,[66] and a maximum likelihood phylogenetic tree with a 500-iteration bootstrap was produced using RAxMLGUI v2.0.[70]

## QUANTIFICATION AND STATISTICAL ANALYSIS

### Behavioral assays

The attraction index of flies in the olfactory trap assays was calculated as (O-C)/(O+C), where O is the number of flies in the Odor trap and C is the number of flies in the solvent trap. Experiments with less than 50% of flies choosing a trap were discarded.

Odorants were classified as attractive, aversive, or neutral if the attraction index was significantly bigger, smaller, or not significantly different from 0, respectively (Two-tailed t test).

The participation index was calculated as (O+C)/# flies in the experimental arena.

### Antennal lobe reconstructions

Glomerular volume was calculated from reconstructed glomeruli and using the information on the voxel size from the laser scanning microscopy scans. Since the total antennal lobe volume differs significantly between species, we normalized the glomerular volume to the antennal lobe's volume before comparing species.

### Calcium imaging analysis

Calcium imaging data were analyzed using FIJI (ImageJ 1.53a National Institutes of Health, USA). Images were corrected for movement using the StackReg Plugin and converted to 8-bit for analysis. All visible glomeruli were manually outlined, established as ROI, and identified as follows: first, glomeruli were discerned in the Z stack performed at the beginning of the experiment by comparison with the 3D AL atlas, and this guided the glomerular identification in the focal plane of excitation; additionally, key glomeruli were recognized thanks to stimulation with diagnostic odorants, and neighboring glomeruli were further identified according to size, shape, position in the AL and position relative to the diagnostic glomeruli. The mean fluorescence was measured for each ROI in all 40 frames. Later, we calculated $\Delta F/F$ by first subtracting averaged values of frames 0 to 8 (pre-odor stimulation, fluorescence background) and then normalizing each $\Delta F$ to the raw fluorescence signal. The peak $\Delta F/F$ was defined as the mean of the 6 frames with the maximum response during the odor application period, which could vary between species and samples. In some cases, the responses in the glomeruli were so strong that the signal clearly covered the neighboring glomeruli, and we discarded those glomeruli from the analysis.

The false color-coded images (Figure 4) were generated in FIJI by subtracting the basal background (average Z projection of frames 1 to 8) and later calculating the mean response of frames 10 to 16. All images of one species correspond to the same experiment. A 16-color scale was applied to each image in a way that at least one pixel of the selected pictures for each species has a maximum value. As a consequence, for the false color-coded images, only a comparison of the responses within species is correct. For further analysis, data were normalized in a way that the comparison between species was valid.

The overall signal intensities vary significantly between species, probably due partially to differences in the expression of GCaMP6f protein. To compare between species and between replicates, $\Delta F/F$ was corrected first by subtracting solvent responses and later normalizing by the maximum response of each experiment.

Heat maps ($\Delta F/Fnorm$) were generated in GraphPad using the mean responses for each odorant/glomeruli combination in all five species. The same scale was used for the five heat maps.

A hierarchical cluster analysis of odor responses between species (Figure 6E) and within each species (Figure S4) was generated in InfoStat using Euclidean distances and Single Linkage.

For the case of comparisons within species, non-normalized $\Delta F/F$ for all glomeruli was used (Figure S4). Pairwise correlations of odor responses within species (Pearson correlation) were calculated. We compared the average Pearson correlation from odorant pairs that have the same valence (either both attractive, both aversive, or both neutral) vs. those that have different valence (attractive-aversive, attractive-neutral, aversive-neutral) via a corrected t test.

We performed pairwise correlations to directly compare each odor response (19 comparisons) in all possible pairs of species (10 pairs in total). In each of the 10 pairs of species, we first calculated for each odorant the Pearson Correlation of the odor coding (using the average responses for the 24 glomeruli). Then, we group odorants with conserved valence between the two species and those with a changed valence and compare the Pearson Correlations via a corrected t test (Figure S5A). A similar approach was used to compare odorants emanating from different sources (Figure S5B).

The mean responses ($\Delta F/Fnorm$) of the main responsive glomeruli in *D. simulans*, *D. sechellia*, *D. suzukii*, and *D. mojavensis* were compared against *D. melanogaster* responses (Figure 5). We considered "main responsive glomeruli" as those that showed at least 5% of the total response for that odorant in at least one of the five species.

Glomerular correlations were calculated for each species against *D. melanogaster* by comparing the mean responses to all odorants for a given glomerulus in both species.

### Statistical analysis and figure preparation

Statistical analyses were performed with the GraphPad Prism 9.0.2 software (Graphpad) and InfoStat package version 2009 (Grupo InfoStat, FCA, Universidad Nacional de Cordoba, Argentina). Normality was tested using the Shapiro-Wilks test, and the homogeneity of variance was assessed graphically by analysis of Homoscedasticity plots (absolute residual vs. predicted values). $p < 0.05$ was considered statistically significant.

The statistical tests and special requirements for each experiment are detailed in the legends of the corresponding figures.

Figures were prepared using a combination of FIJI, Graphpad, Microsoft Excel 2016, FigTree, Adobe Photoshop, and Adobe Illustrator CS5.